UNIVERSITY OF THESSALY

SCHOOL OF ENGINEERING

DEPARTMENT OF MECHANINCAL ENGINEERING

JET MULTIPHASE FLOW- EROSION DUE TO PARTICLE IMPACTS

by

IOANNIS STAVROS PANAGIOTOPOULOS

Submitted in partial fulfillment of the requirements for the degree of Diploma in Mechanical Engineering at the University of Thessaly

Volos, 2025

UNIVERSITY OF THESSALY

SCHOOL OF ENGINEERING

DEPARTMENT OF MECHANINCAL ENGINEERING

JET MULTIPHASE FLOW- EROSION DUE TO PARTICLE IMPACTS

by

IOANNIS STAVROS PANAGIOTOPOULOS

Submitted in partial fulfillment of the requirements for the degree of Diploma in Mechanical Engineering at the University of Thessaly

Volos, 2025

Approved by the Committee of Final Examination:

Advisor Dr.Konstantinos Ritos

Assistant Professor, Department of Mechanical Engineering, University of Thessaly

Member Prof. Bontozoglou Vasileios

Professor, Department of Mechanical Engineering, University of Thessaly

Member Prof. Papathanasiou Athanasios

Professor, Department of Mechanical Engineering, University of Thessaly

Ευχαριστίες

Θα ήθελα να ευχαριστήσω τον επιβλέποντα καθηγητή μου Κωνσταντίνο Ρήτο για την πολύτιμη και αδιάκοπη βοήθεια και καθοδήγηση του, καθώς και για την άψογη συνεργασία και το ενδιαφέρον που έδειξε κατά τη διάρκεια της εκπόνησης της διπλωματικής μου. Ακόμα ευχαριστώ τον διδακτορικό φοιτητή Jonathan Proctor για την προθυμία του να παρέχει βοήθεια και την επίλυση αποριών που δημιουργήθηκαν κατά την μελέτη μου. Ευχαριστώ επίσης τον Σταύρο Παντόπουλο που ήταν πάντα δίπλα μου καθ όλη την διάρκεια των σπουδών μας.

Οφείλω τέλος να ευχαριστήσω την οικογένεια μου και να τους αφιερώσω την διπλωματική μου εργασία, καθώς με στηρίζουν όχι μόνο στις σπουδές μου αλλά και σε όλους τους τομείς της ζωής μου.

Ιωάννης-Σταύρος Παναγιωτόπουλος

JET MULTIPHASE FLOW- EROSION DUE TO PARTICLE IMPACTS

Ioannis-Stavros Panagiotopoulos

Department of Mechanical Engineering, University of Thessaly

Supervisor: Dr. Konstantinos Ritos

Abstract

Multiphase jet impingement flows play a critical role in various industrial applications, including cooling systems, material processing, and erosion prediction in engineering structures. A number of different turbulence modeling approaches were compared in order to simulate the flow of a variety of jet impingement cases, using ANSYS Fluent 2024 R2. Initially, a 2D jet impingement case was simulated using SST k-ω, RNG k-ε, and RNG k-ε with enhanced wall treatment, with Velocity magnitude, Axial velocity, and Radial velocity compared at a height 1 mm above the plate. A 3D case, based on an experimentally validated submerged jet impingement geometry, was then analyzed using RNG k-ε with enhanced wall treatment, SST k-ω, and Reynolds Stress Models (RSM). Next, a validated jet impingement case with slightly different geometry was examined. A 2D and a 3D simulation were conducted, with Velocity magnitude contours compared against experimental data. Additionally, a symmetry-based analysis was performed, comparing full, half, and quarter geometries, as well as 15°, 30°, and 45° splines. The study then extended to liquid-solid multiphase flow simulations to predict erosion depth and distribution on the impinged plate. Further analysis examined the effect of changing inlet velocity on erosion intensity, demonstrating a clear analogy between velocity increase and erosion depth. Additionally, inclined plates (15°, 30°, and 45°) were simulated, in order to compare the differing velocity magnitude contours and erosion distribution patterns. The need for higher result resolution was underlined and a revised methodology was undertaken in order to improve quality while maintaining compliance with the limitations of the problem. By comparing numerical results with experimental data, this research provides insights that contribute to the advancement of CFD-based erosion modeling and flow analysis. These simulations can hopefully provide conclusions that enhance the accuracy and applicability of CFD simulations in industrial settings.

Key Words: Turbulence modeling approaches, Multiphase Jet Impingement Flows, Erosion Prediction

ΠΟΛΥΦΑΣΙΚΕΣ ΡΟΕΣ ΠΙΔΑΚΑ- ΔΙΑΒΡΩΣΗ ΛΟΓΩ ΠΡΟΣΚΡΟΥΣΗΣ ΣΩΜΑΤΙΔΙΩΝ

Ιωάννης-Σταύρος Παναγιωτόπουλος

Τμήμα Μηχανολόγων Μηχανικών, Πανεπιστήμιο Θεσσαλίας

Επιβλέπων Καθηγητής: Κωνσταντίνος Ρήτος

Περίληψη

Οι πολυφασικές ροές προσπίπτοντος πίδακα παίζουν σημαντικό ρόλο σε διάφορες βιομηχανικές εφαρμογές, συμπεριλαμβανομένων των συστημάτων ψύξης και επεξεργασίας υλικών και στην πρόβλεψη της διάβρωσης σε μηχανολογικές κατασκευές. Συγκρίθηκαν διάφορες προσεγγίσεις μοντελοποίησης της τύρβης για την προσομοίωση της ροής ποικίλων περιπτώσεων προσπίπτοντος πίδακα, χρησιμοποιώντας το λογισμικό ANSYS Fluent 2024 R2. Αρχικά, προσομοιώθηκε μια δισδιάστατη περίπτωση προσπίπτοντος πίδακα με χρήση των μοντέλων SST k-ε, RNG k-ε και RNG k-ε με ενισχυμένη επεξεργασία τοιχωμάτων, όπου συγκρίθηκαν το μέτρο της ταχύτητας, η αξονική ταχύτητα και η ακτινική ταχύτητα σε ύψος 1 mm πάνω από την πλάκα. Στη συνέχεια, αναλύθηκε μια τρισδιάστατη περίπτωση, βασισμένη σε πειραματικά επικυρωμένα δεδομένα, χρησιμοποιώντας τα μοντέλα RNG k-ε με ενισχυμένη επεξεργασία τοιχώματος, SST k-ω και Reynolds Stress Model (RSM). Έπειτα, εξετάστηκε μια επικυρωμένη περίπτωση προσπίπτοντος πίδακα με ελαφρώς διαφορετική γεωμετρία. Πραγματοποιήθηκε προσομοίωση 2D και 3D, με σύγκριση των γραφημάτων μεγέθους ταχύτητας με πειραματικά δεδομένα. Επιπλέον, πραγματοποιήθηκε ανάλυση με βάση τη συμμετρία, όπου έγινε σύγκριση των αποτελεσμάτων που προέκυψαν σχεδιάζοντας ολόκληρη την γεωμετρία, την μισή , το ένα τέταρτο, καθώς και ‘’φέτες’’ 15°, 30° και 45°. Στη συνέχεια, η μελέτη επεκτάθηκε σε προσομοιώσεις πολυφασικής ροής υγρού-στερεού με στόχο την πρόβλεψη του βάθους και της κατανομής της διάβρωσης στην προσκρούουσα πλάκα. Περαιτέρω ανάλυση έγινε με επίκεντρο την επίδραση της μεταβολής της ταχύτητας εισόδου στην ένταση της διάβρωσης, καταδεικνύοντας μια σαφή αναλογία μεταξύ της αύξησης της ταχύτητας και του βάθους διάβρωσης. Επιπλέον, προσομοιώθηκαν κεκλιμένες πλάκες (15°, 30° και 45°), προκειμένου να συγκριθούν τα διαφορετικά γραφήματα μεγέθους ταχύτητας και τα μοτίβα κατανομής της διάβρωσης. Κατά την διάρκεια των προσομοιώσεων αναδύθηκε η ανάγκη για βελτίωση της ποιότητας των αποτελεσμάτων και μια αναθεωρημένη μεθοδολογία υιοθετήθηκε, για αυτό το σκοπό, τηρώντας πάντα τους περιορισμούς της φύσης του προβλήματος. Συγκρίνοντας τα αριθμητικά αποτελέσματα με πειραματικά δεδομένα, η παρούσα έρευνα παρέχει πληροφορίες που συμβάλλουν στην πρόοδο της μοντελοποίησης της διάβρωσης και της ανάλυσης ροής με βάση λογισμικά CFD. Οι προσομοιώσεις αυτές μπορούν, ελπίζουμε, να παράσχουν συμπεράσματα που θα βελτιώσουν την ακρίβεια και τη δυνατότητα εφαρμογής των προσομοιώσεων CFD σε βιομηχανικές περιστάσεις.

Λέξεις-Κλειδιά: Προσεγγίσεις Μοντελοποίησης Τύρβης, Πολυφασικές Ροές Προσπίπτοντος Πίδακα, Προσομοίωση Διάβρωσης

Contents

List of Figures

Chapter 1: **Introduction**

1.1 Background and Motivation

Multiphase flows are extensively encountered in a wide range of industrial processes, including oil and gas transportation, fluidized bed reactors in chemical engineering, cooling of electronic components via jet impingement, abrasive slurry transport in mining, and fuel injection in internal combustion engines. These processes are often critical to the efficiency, safety, and reliability of industrial systems, further underscoring the importance of precise flow modeling. These systems involve complex interactions between different phases (typically liquids, gases, and solid particles) which makes accurate prediction of flow behavior and surface degradation particularly challenging.

1.2 Single Phase Flow and Turbulence Modeling Approaches

Before attempting to simulate the way multiphase flows behave in jet impingement cases, there is the need to determine an accurate foundation by predicting the single phase flow of water in such a geometry. Establishing this baseline is essential not only for validating numerical models but also for ensuring that subsequent multiphase simulations are built upon a robust and verifiable understanding of the flow dynamics. Turbulence is generally a disordered, unstable, three dimensional phenomenon, distinguished by high Reynolds Numbers and swirl fluctuations, making it difficult to predict. This chaotic nature of turbulence leads to significant computational challenges, necessitating the development of specialized mathematical techniques and approximations. The inherent complexity in predicting such a chaotic motion of fluids, has led to the development of numerous different turbulence modeling approaches all based on the common principal of decomposing the flow into different components and individually applying the Navier-Stokes and continuity equations to each one of them. The procedure of splitting the flow into distinct components is known as averaging. Many averaging procedures have been developed over the years with Reynolds-Averaged Navier-Stokes (*RANS*), being the one most commonly used by CFD software. RANS divides the flow into mean and fluctuating variables. However there are different ways of dividing the flow for example splitting it into large and small length scales or eddy sizes, a process called Large Eddy Simulation (*LES*). Following the application of time or space averaging some unresolved terms called Reynolds stresses are introduced into the Navier-Stokes Equations. In order to resolve them a number of sets of Partial Differential Equations (*PDEs*) called eddy viscosity models have been developed, such as k-ε and k-ω models just to name a few. Each model comes with its own strengths and limitations, and the careful selection of the appropriate one is crucial depending on the characteristics of the simulated flow and given geometry. Most of these models will be assessed and directly compared to one another in a number of different cases in this thesis.

1.3 Pipe Erosion in Multiphase Flows

Another point of interest when dealing with Multiphase Flows through pipes and particularly with liquid-solid flows is predicting the erosion depth on the pipe walls. Deciding on the most suitable combination of mesh, eddy viscosity and erosion models to be employed on different cases of boundary conditions or pipe angles is critical to ensure precise and accurate calculations and predictions of total erosion depth and pattern on pipe walls and surfaces.

Each model comes with its own strengths and limitations, and the careful selection of the appropriate model is crucial depending on the characteristics of the simulated flow. This would be useful for a number of real world industrial scenarios. Having reliable models to predict erosion would help prevent an unexpected pipe failure or rapture and schedule the mechanical maintenance frequency. If combined with material technology it could even help take some design decisions like pipe material and pipe thickness. Thus, the insights gained through detailed CFD simulations could guide not only maintenance practices but also inform engineering design choices at an early stage.

1.4 Computational Software Used

All the simulations presented were carried out using ANSYS Fluent 2024 R2 student edition. ANSYS Fluent has been the industry standard when it comes to modeling complex fluid flow phenomena, including turbulence, heat transfer, multiphase interactions, and chemical reactions due to its robustness, adaptability and user-friendly environment. Its wide validation base and extensive documentation also make it the preferred choice for both industrial and academic research applications. ANSYS Discovery was utilized to generate all necessary geometries and ANSYS Meshing was employed as the meshing tool for all cases. Another crucial feature that renders ANSYS Fluent the optimal software to encounter multiphase flow erosion simulation, is the User Defined Function (*UDF*) feature, as some of the physics and equations needed to simulate such a complex phenomenon are not included in the standard physics tab. The flexibility offered by UDFs allows researchers to customize boundary conditions, material properties, and source terms, thereby enhancing the fidelity of the simulations beyond the limitations of the default models. UDFs were also used on post processing the results of this thesis when erosion rate had to be transformed into erosion depth.

1.5 Literature Review

Submerged Jet Impingement studies have been the center of attention for many researchers among the years. Some of them have also targeted the simulation of erosion rate and depth of multiphase liquid-solid flows as well. While this paragraph briefly describes some of these studies, there are many more taken into consideration and referred to in this thesis.

In 2024 Mendi Chen et al. (1) proposed the development of a modified drag model for the particles' motion taking into consideration the participation of turbulence intensity as well as a modified erosion model in elbow geometries taking into consideration low-angle impacts. The proposed model enhanced prediction accuracy in both vertical pipe as well as jet impingement cases.

In 2021 Rached-Ben Mansour (2) investigated and measured erosion on a submerged jet impingement case using ANSYS Fluent. They studied how different inlet velocities, nozzle diameters and shapes, nozzle-plate distances, impingement angles and particle sizes influence erosion profiles and patterns. Comparisons with experimental data were also carried out validating the CFD models.

In 2017 Chan Wang et al. (3)focused on studying the behavior of a submerged jet impingement case on different Reynolds Numbers, impingement angles and nozzle diameter to nozzle-plate distance ratios, revealing a clear analogy between the flow characteristics and the parameters above.

In 2014 A.Mansouri et al. (4) did a combined study of CFD and real-world experiments on air-solid and liquid-solid jet impingement cases. Results and measurements were directly compared validating the simulations. Results from this article and the accommodating dissertation are primarily used to validate the CFD results of this thesis.

In 2015 Alasdair MACKENZIE et al. (5)compared different CFD software packages on their accuracy of simulating a submerged impinging jet. Experimental measurements were also done in order to compare the results of different CFD software packages. A similar case with geometry and boundary conditions drawn from this article was designed in this thesis to take advantage of the experimental data provided, to help with validations.

Chapter 2: Turbulence Modeling Approaches

2.1 Introduction to Turbulence

The management and prediction of turbulent flow behavior has been the subject of scientific research for many years and remains one of the major unsolved problems in physics (1).The fact that turbulent flow is generally a disordered, unstable, three dimensional phenomenon, distinguished by high Reynolds Numbers and vorticity fluctuations, is what makes it such a difficult issue to resolve (2).This complexity has led to the development of a large number of turbulence modelling approaches. The majority of these models share the same philosophy of attempting to decompose the chaotic turbulence oscillations, into two or more fundamental components that are easier to handle and applying this discretization to solve the Navier-Stokes equations numerically.

2.2 Categorization of Navier Stokes equation solving methods and Turbulence Modeling Approaches

Over the years a number of different models to approach the prediction of turbulent flows have been developed, each with both advantages and disadvantages (*i.e. being better at predicting flows with flow separation or sudden directional changes, but expensive in terms of simulation costs* (3)). The three main methods of solving the Navier-Stokes equations are: Reynolds-Averaged Navier Stokes (RANS), Large Eddy Simulation (LES) and Direct Numerical Simulation (DNS), with RANS having emerged as the main turbulence modeling approach for Computational Fluid Dynamics (CFD) software, due to its ability to accurately enough predict a large number of different cases, with minimal grid requirements (2) (4).

2.2.1 Reynolds Averaged Navier-Stokes Equations (RANS)

Reynolds-Averaged Navier Stokes (RANS), named after its founder Osborne Reynolds, aims to solve the Navier Stokes equations by dividing the flow variables into mean and fluctuating, through a process called time-averaging or Reynolds-averaging. After Reynolds-averaging, the Navier Stokes equations are transformed into the following expressions for a two-dimensional flow:

$$\rho u \frac{du}{dx} + \rho v \frac{du}{dy} = -\frac{dp}{dx} + \frac{d}{dy}\left[\mu \frac{du}{dy} - \rho \overline{u'v'}\right]$$

$$\rho u \frac{dv}{dx} + \rho v \frac{dv}{dy} = -\frac{dp}{dy} + \frac{d}{dy}\left[\mu \frac{dv}{dy} - \rho \overline{u'v'}\right]$$

where the velocity terms are time-averaged (*generally shown as $\bar{x}$, but on the above expression the bars have been dropped for simplicity*)and u',v' are the fluctuating (*time-varying*) quantities (1).

As seen above after Reynolds-averaging an extra term is added to the Navier-Stokes equations ($-\rho\overline{u'v'}$). This term is called Reynolds stress. Modeling the Reynolds stresses is necessary to completely resolve the Reynolds-averaged Navier Stokes equations. This is known as the closure problem and it is the reason why the different turbulence models that will be presented later, needed to arise.

2.2.2 Large Eddy Simulation (LES)

Large Eddy Simulation (LES), is derived after considering the flow to be split into small and large –length scales (*eddy sizes*) through a process known as spatial filtering (1). Similarly to RANS, while large eddy sizes can be computed numerically, the existence of small eddy sizes causes an additional term to appear after spatial filtering the original equations in two dimensions:

$$-\rho(\overline{uv} - \bar{u}\bar{v})$$

Resolving these extra terms requires the implementation of models called subgrid-scale models. Amongst the variety of subgrid-scale models that have been developed throughout the years, the most widely known are the Smagorinsky model, two-point closure models and one-equation models (5).

2.2.3 Direct Numerical Simulation (DNS)

Direct Numerical Simulation (DNS), avoids any time or scale averaging or any model implementation and proceeds to fully resolve the Navier Stokes equations, providing the most detailed results no matter the complexity of the flow or the geometry. However it is understandable that DNS, by not applying any of the RANS or LES simplifications, drastically increases the computational cost, in many cases even by a ratio of Re^3in terms of time steps (6). This leads to DNS being avoided for any industrial applications, except for some cases with very low Reynolds number flows, while it is currently mainly used to help provide data to improve the existing RANS models (7).

Comparing these methods of solving the Navier Stokes equations and choosing which one to use is highly depended on the characteristics of each case and the equipment available. In general RANS is the most complete method, combining both speed and accuracy for a variety of problems. LES can be considered a compromise between DNS and RANS, being more costly in terms of computations than RANS, however proving to be superior in terms of information in some cases (2).

Figure 1.gives a better understanding of how each method of solving the Navier Stokes equations and the corresponding turbulence modeling approach is categorized (1).

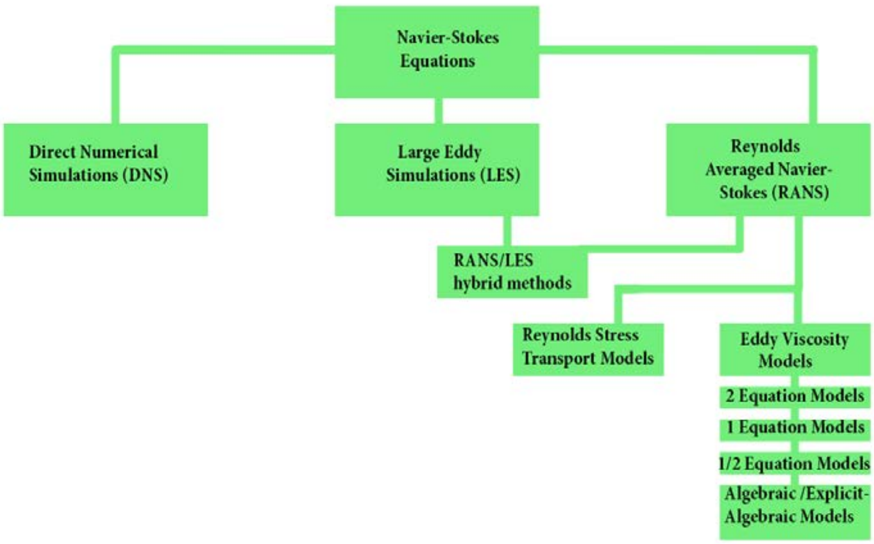

Figure 1: Categorization of Navier Stokes equations solving and turbulence modeling approaches

2.3 RANS Turbulence Models

Having established that RANS is the current industry standard for solving the Navier Stokes equations with CFD software, it is important to further analyze the turbulence models that have been developed over the years to resolve the Reynolds stresses that appear after time averaging. One way to approach this problem is to directly solve the Reynolds stresses through a method known as Reynolds stress models (RSM) or Reynolds stress transport models. In three dimensional problems however, directly solving for the Reynolds stresses requires the solution of seven different equations, (*six for the different Reynolds stress tensors and one for the turbulence dissipation*) making RSM an unattractive option (7).

This is where turbulence modeling needs to be implemented. Most of the models developed are based in the assumption that the Reynolds stress is equivalent to the mean strain rate, known as the Boussinesq eddy viscosity approximation or (5):

$$\tau_{ij} = \mu_t \left(\frac{d\bar{u}_i}{dx_j} + \frac{d\bar{u}_j}{dx_i} \right) - \frac{2}{3}\bar{\rho} k \delta_{ij}$$

Where k is the kinetic energy of the turbulent fluctuations, expressed as:

$$k = {}^{1}/_{2}\,(\overline{u'^2} + \overline{v'^2} + \overline{w'^2})$$

and μ_t is the turbulent viscosity, given by the turbulence models known as eddy viscosity models (1).

2.4 Eddy Viscosity Models

Eddy viscosity models are generally categorized by the number of partial differential equations (PDEs) needed in order to resolve them (*as shown in Figure 1.*) (1). Although these models are designed to solve the same problem, they approach it with many different ways, thus they end up having differences in the results and the computational power they need, making each model more suitable for different cases. Of the many models available the one with the most recommendations for the majority of industrial purposes is the Shear Stress Transport model (*k-ωSST*) (2) (6), due to its ability to accurately predict different types of flows with adverse pressure and velocity gradients and its high-level wall treatment. k-ω SST is a two-equation eddy viscosity model. However there are several other model that are also widely used and are in some cases superior to k-ω SST.

2.4.1. One Equation Models

The Spalart-Allmaras (SA) eddy viscosity model is a one equation model commonly preferred for aeronautical applications, due to its simplicity of only having to solve one partial differential equation, making it attractive for external flows with adverse pressure gradients and dense meshes. However its separation predicting ability is lower than two-equation models like k-ωSST (1).

2.4.2 Two Equation Models

The two-equation models have been the standout models for simulating any industrially applicable flow. The k-εmodels are a great alternative when backwards compatibility is desirable. These models are also split into:

- the Standard k-ε Model, most frequently used when a ''Production Limiter'' is activated, in order to handle cases with excessive turbulence. It is highly dependent on the mesh type (*coarse or fine*) and scalable wall functions are recommended (2).
- the Realizable k-εModel (RKE), also mesh dependent and unstable when it comes to predicting turbulence (2).
- the Re-Normalization Group RNG k-ε Model (RNGKE) is the most preferred k-ε model, being able to calculate smaller scales of motion than the Standard and Realizable k-ε, making it more suitable even than the SST k-ωmodel in some cases (*i.e. indoor air flows or rotating cavities*) (2).

As mentioned SST k-ω model is the most widely used eddy viscosity model currently used in the industry. The term k-ω derives from the two transported variables included in the model's equations. k is the variable for kinetic turbulent energy, accounting for the energy in the turbulence and ω the specific dissipation, accounting for the scale of the turbulence (5).

The standard k-ω model is a two equation model that relies on transporting the equations for the turbulent kinetic energy k and the turbulent dissipation rate ω (5). In order to overcome the shortcomings of the standard k-ω model many revisions have been made, with SST k-ω being the superior (8). ANSYS even suggests avoiding the standard method completely, as it highly depends in the free stream ω values, referring that it's availability is still there only for historical reasons (2).

Also worth mentioning is the Generalized Kappa Omega (GEKO) model, a model that allows it's user to ''tune'' it by determining its variables making it a hybrid between the SST k-ω and k-ε models. Finally the Wallin-Johansson Explicit Algebraic Reynolds Stress Model (WJ-EARSM) is a model chosen when secondary flows are relevant, it is however vulnerable to streamline curvature (2).

2.4.3 Reynolds Stress Models

Reynolds Stress Models (RSM) are 7-equation models also known as Reynolds Stress Transport Models (RSTM), used to fully resolve complicated geometries or non-ideal grids (i.e. cases with sudden geometry changes or system rotation), by solving the exact Reynolds Stress transport equation. RSM uses 6 transport equations to solve for the Reynolds Stress Tensor Components and 1 transport equation for the Dissipation rate, thus giving more detail on how turbulence is distributed at the cost of larger computational demands. Therefore RSM is only recommended for cases with higher precision demands or cases where RSM has shown better results than the regular eddy viscosity models. ANSYS also recommends combining the use of RSM models with the omega equations, creating the GEKO-RSM model.

2.4.3.a RSM Submodels

When opening the Reynolds Stress Models (RSM) dialogue in ANSYS Fluent, you are given a choice regarding which submodel you want to work with. For instance you can choose between the Linear Pressure –Strain, the Quadratic Pressure- Strain and the Low- Reynolds Stress- Omega Models.

The Linear Pressure- Strain Model is the default model for ANSYS Fluent. This model assumes linear redistribution for the turbulence kinetic energy. It produces accurate results for most cases of turbulence modeling with moderate to high Reynolds numbers (9). This model however is not recommended for flows with abrupt geometry changes or in cases with strong secondary flows (9).

The Quadratic Pressure- Strain Model can improve the accuracy of the results in cases where the Linear Pressure- Strain Model comes short, by including quadratic (non-linear) terms in the pressure-strain coupling (9). This allows the model to be used for more complex cases, in the cost of being more computationally expensive than the linear model (2) .

The Low- Reynolds Stress Omega Model is an RSM submodel based on anω-formulation instead of the typical ε-equation of the k-εmodels. As the name implies this model provides greater accuracy for flows with low Reynolds Numbers (9). If chosen it is recommended that it is combined with the low- Reynolds correction option in order to correctly capture the turbulence dissipation near the walls. The downside of the method is that there may be overestimations for the turbulence levels in free-stream regions (2).

2.4.3.b Submodel Tuning

In ANSYS Fluent, users can adjust model constants to fine-tune both the Linear and Quadratic Pressure-Strain Models. Constants C_1 and C_2, which govern the redistribution of turbulent kinetic energy, are set by default to 1.44 and 1.92 respectively (10). Increasing these values intensifies the energy redistribution, potentially altering flow behavior predictions. Another tunable parameter is C_μ, the dissipation rate constant, which controls how quickly turbulent energy decays. Its default value is 0.09, with higher values promoting faster energy dissipation and lower turbulence intensity (9).

When working with the Low- Reynolds Stress Omega Model, aside of the C1 and C2 constants, two more constants are offered for change. The Alpha Infinity (a_∞) and Alpha- Star Infinity (a^*_∞) constants are used to modify the k-ωturbulence model. a_∞ affects the transition of the model from wall- bounded to free stream conditions, influencing the rate of production and dissipation balance in the turbulence equations. a^*_∞ affects the dissipation rate of turbulence kinetic energy in the freestream regions (9).

2.5 Production Limiters and Enhanced Wall Treatment

2.5.1 Production Limiters

The implementation of Production Limiters is crucial when encountering two-equation turbulence models (2). When applying the Boussinesq eddy-viscosity assumption, a quadratic term is added to the equation of the kinetic energy (*k-equation*). This can cause the turbulent kinetic energy to be overestimated in regions with adverse velocity gradients or in stagnation and acceleration zones (5). Enabling the production limiter in cases where it is not automatically enabled (*i.e. the majority of k-ε models, while all ω-equations have a* *production limiter on by default*), prevents unrealistic energy growth and improves model stability (2).

2.5.2 Enhanced Wall Treatment

Enhanced Wall Treatment is applied when greater quality is required in the near wall regions, where the phenomena observed are more complicated. Enabling the enhanced wall treatment implements a logarithmic velocity profile to approximate the velocity, alternating with fully resolving the velocity equations depending on whether the mesh is fine enough or not.

Chapter 3: Comparisons of Different Eddy Viscosity Models in Jet Impingement Cases

3.1 First Jet Impingement Case

SST k-ω, RNG k-ε and RNG k-εwith enhanced wall treatment and a production limiter were compared when simulating the flow in a jet impingement case, using ANSYS Fluent 2024 R2 student edition. The geometry used for the simulation consisted of a 45 mm long tube with a diameter of 8 mm and 80X48mm sidewalls (11).

3.1.1 Mesh Setup and Quality Metrics

In order to create the mesh, edge sizing was applied to all the edges of the geometry using the method of number of divisions with a bias factor of 2.0, while face meshing was also implemented in order to keep the geometry of the mesh elements steady. This resulted in a mesh of 58,37% minimum quality, with the majority of the mesh elements having a quality of over 95%. Figure 2 shows a representation of the mesh with element quality enabled.

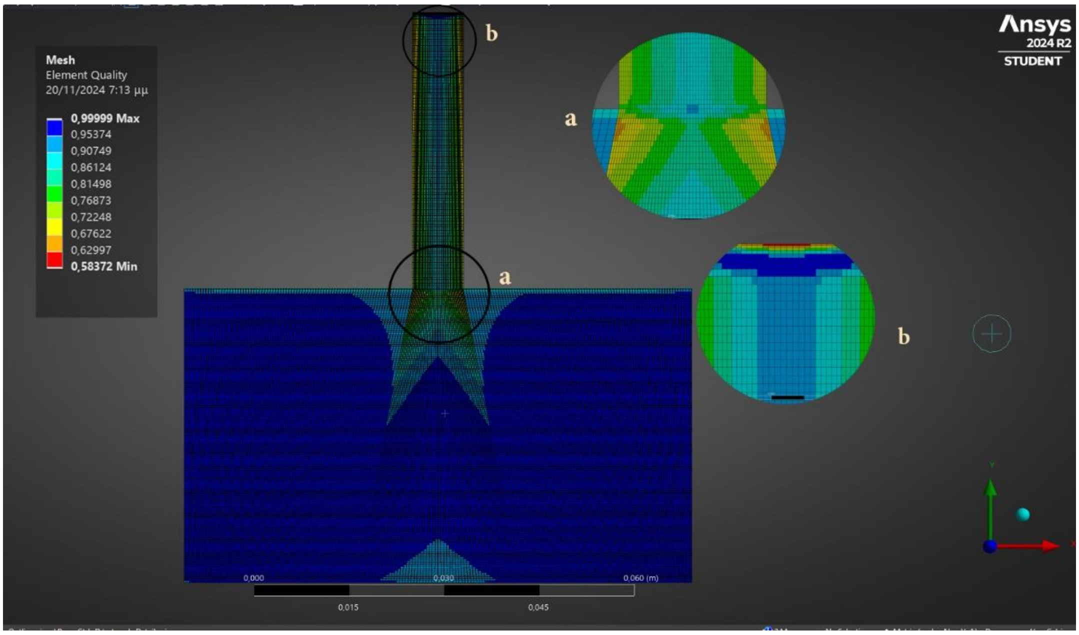

Figure 2: Element quality for the mesh used to simulate the jet impingement case

The regions where the lower quality elements are spotted have been scaled up in the above figure to show that they are small in number relative to the higher quality cells and even though their quality of 58.37% at worst is still more than acceptable these cells are also placed in regions where we do not expect the flow to have major turbulences so the final results will not be affected.

3.1.2 Fluent Setup

For the solution setup, a 2D ANSYS Fluent environment was used for all simulations, with water-liquid as the working fluid, the properties of which, were copied from the fluent library. The inlet velocity was set to 14m/s and no slip condition was used for the sidewalls (11). Standard initialization with inlet boundary condition was implemented and the absolute criteria for the residuals in order for the solution to be converged were changed to 1e-6. For the case of SST k-ω, parameters were set to default with the production limiter also being enabled by default and set with a clip factor of 10. In the case of RNG k-εstandard wall functions were used and the parameter values were set to default, while in the case of RNG k-ε EWT (*enhanced wall treatment*) the enhanced wall treatment function was activated along with a production limiter with a clip factor of 10.

3.1.3 Results and Comparisons

The results compared were the Velocity Magnitude, the Radial Velocity and the Axial Velocity, at a line 1mm above the bottom plate.

The results, in the form of graphs, are shown in Figure 3.

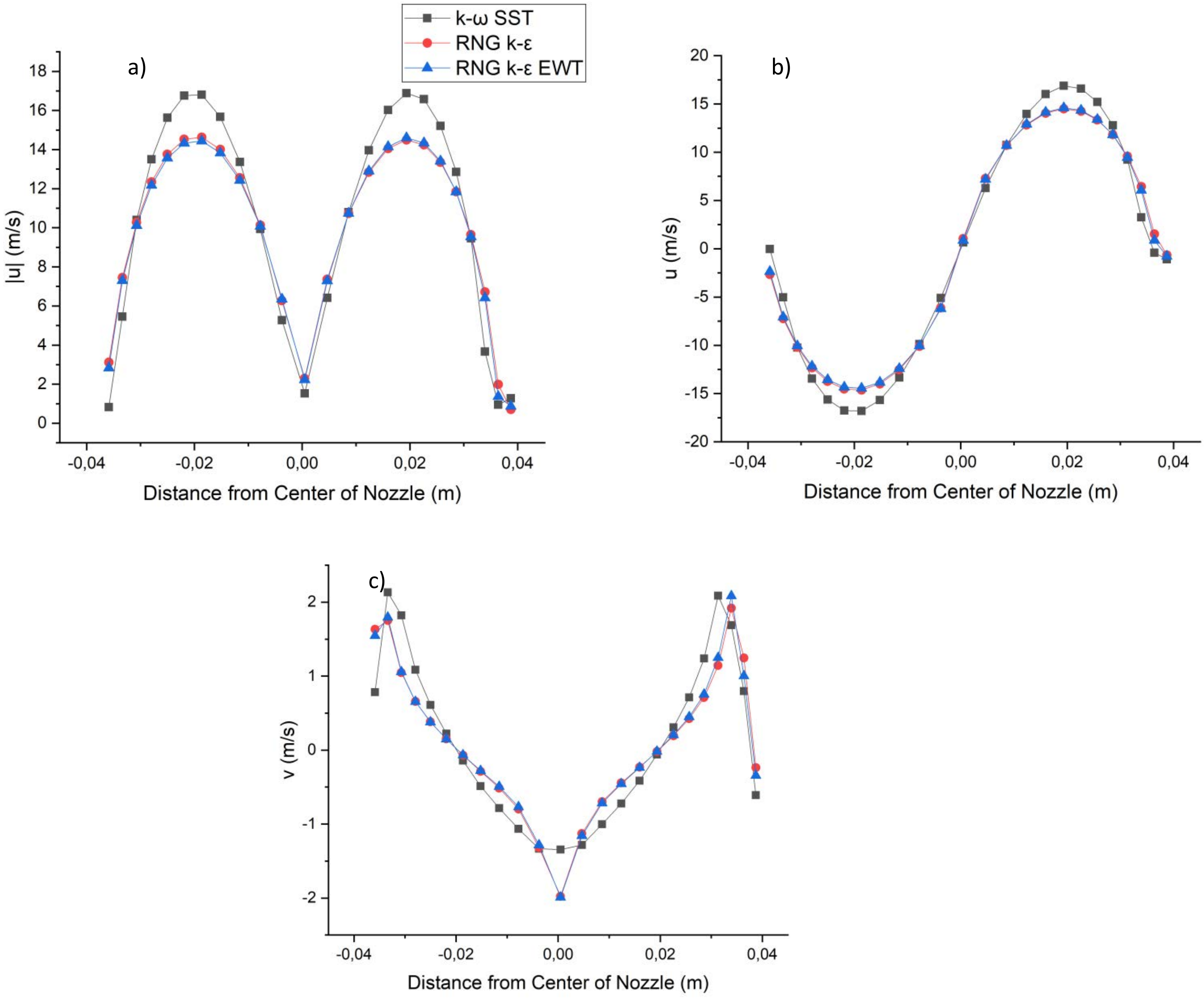

Figure 3: Graphs for the Velocity Magnitude (a), the Radial Velocity (b) and the axial Velocity (c) 1mm above the bottom plate, using k-ω SST, RNG k-ε and RNG k-εwith enhanced wall treatment

Out of the three models used the one showing any modulation is the k-ω SST Eddy Viscosity Model, when predicting the Velocity Magnitude and Radial Velocity at a distance around 2 mm away from the center of the Nozzle and when predicting the Axial Velocity near the stagnation point. RNG k-ε and RNG k-ε with enhanced wall treatment didn't give any fluctuations between them, meaning that enhanced wall treatment isn't necessary when simulating the flow in this case. The deviation of k-ω SST compared to the other two could actually suggest that k-ω SST was better at predicting turbulence intensity, something that would agree with the theoretical point made earlier.

3.2 CFD Validation MACKENZIE experiments

In order to compare the different Turbulence Modeling Approaches with experimental data provided by Alasdair MACKENZIE et. Al. at their article titled **'' A COMPARISON OF CFD SOFTWARE PACKAGES' ABILITY TO MODEL A SUBMERGED JET"** (12), a geometry of the same dimension as those proposed in the experiment carried out was created and imported in ANSYS Fluent using ANSYS Discovery. Then SST k-ω, Reynolds Stress Model (*RSM*) and RNG k-εturbulence models were all used to solve the problem and the results were compared with the experimental measurements provided by the article in study.

3.2.1 Geometry Setup

Inlet Diameter was set at 8mm, the distance between the pipe exit and the 25mm wide wall specimen was 12,8mm all matching the dimensions of the experimental set up. Pipe length was set at 100 mm long in order to ensure the flow would be fully developed before reaching the pipe outlet. Half the array was modeled, using symmetry both in the fronts and sides of the geometry to calculate the rest of the control volume, in order to reduce the number of elements and the computational power needed to solve the problem.

3.2.2 Mesh Setup and Quality Metrics

In order to create the mesh for this geometry, Fluent Meshing was employed, with a Sweep Method applied to force an orthogonal mesh around the body and face meshing on the surfaces requiring a mapped mesh. A Body Sizing Method was also implemented to refine the mesh near the specimen, as the area of interest was located a few millimeters above it and the results required greater accuracy. This was achieved by implementing the Sphere of Influence Method. The center of the sphere was set to be at the center of the specimen, the sphere had a radius of 5mm and the refined element size was set at 0.1mm.The final number of nodes came to 96,008 and the minimum orthogonal quality was above 30%, with most elements being close to 100% quality.

3.2.3 ANSYS Fluent Setup

ANSYS Fluent was used to setup and solve the problem, with Double Precision enabled and 4 Parallel Processors used to achieve better result quality. Inlet boundary condition was set for velocity Inlet, with a speed of 2.5m/s and the turbulence specification method used was Intensity (*1%*) and Hydraulic Diameter. Symmetry and No Slip conditions were applied for the fluid domain and the Walls respectively, while Pressure Outlet boundary conditions were used on the outlets with an Absolute Gauge Pressure of 0 Pa. Water of 998.2 kg/m^2 density and 0.001003 kg/m*s viscosity was used as the working fluid. Pressure and Velocity were coupled using the SIMPLE Scheme with Second Order Upwind Spatial Discretization, in order to improve the results' quality. The residuals' absolute criteria were set at 1e-06. These settings were kept steady for all the methods used (*SST k-ω, RSM, RNG k-ε*).

3.2.4 Results and Comparison

The results were then plotted side by side and compared with the experimental data provided in the article. Plot digitizer software was used to extract the experimental data and Origin was used to plot everything together. The results for the Velocity Magnitude, the Radial and Axial Velocities for each method compared with the experimental data are shown on Figure4.

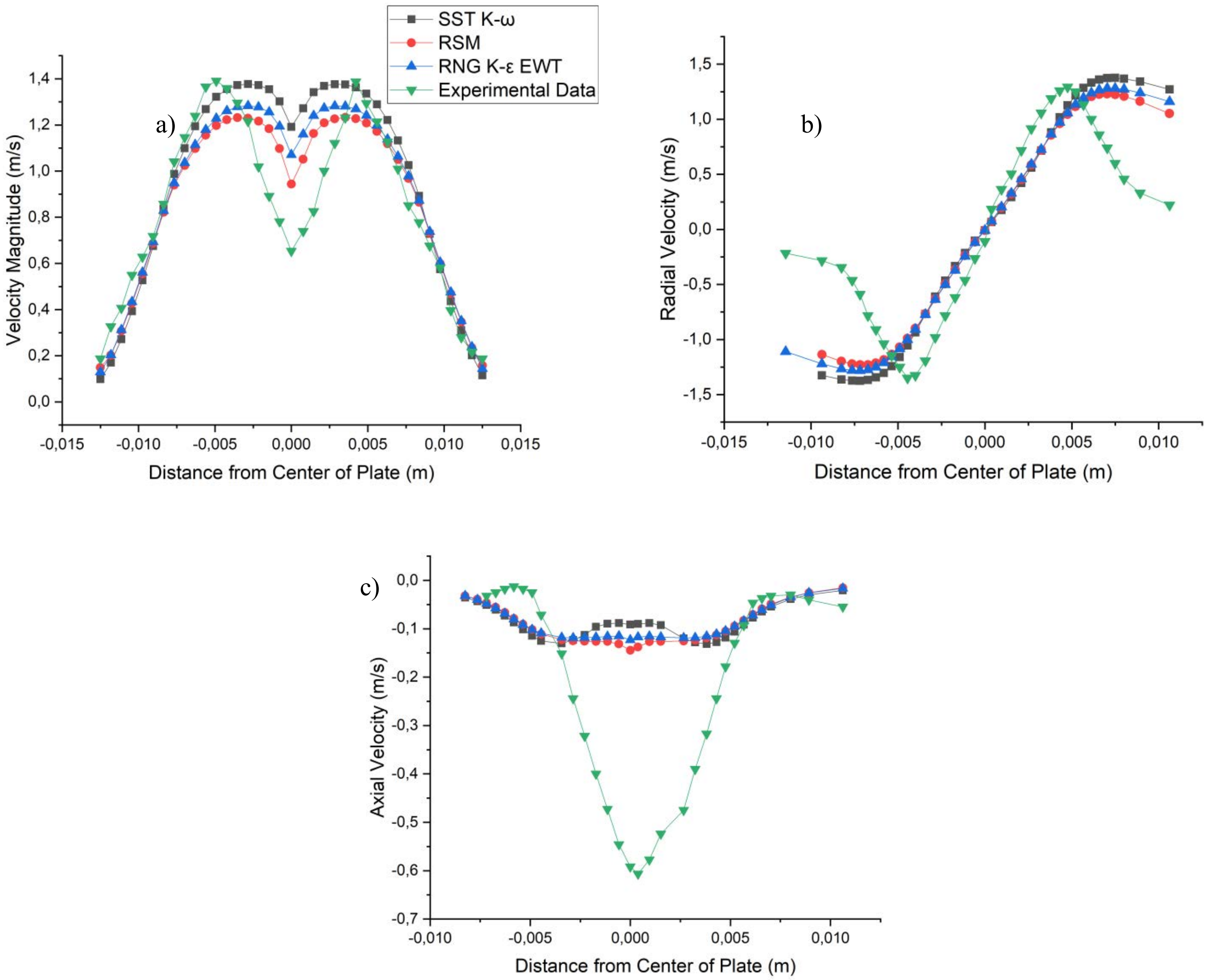

Figure 4: Graphs for the Velocity Magnitude (a), the Radial (b) and the Axial (c) Velocities 1mm above the bottom plate, using SST k-ω, RSM and RNG K-ε with Enhanced Wall Treatment, compared with Experimental Data

After observing the results we can determine that the Reynolds Stress Model is the most reliable turbulence modeling method for this case. All methods had difficulties predicting the Axial Velocity and consequently the Velocity Magnitude near the center of the plate. This could be caused by the anisotropy of the flow near the stagnation point, given the fact that most turbulence models assume isotropic turbulence behavior. Grid sensitivity issues could also cause similar issues and Near-Wall inflations could be worth trying. However RSM came closer to accurately predicting the reduction in Velocity near the center, but also the behavior of the Radial Velocity at the edges of the plate. Based on those observations we can conclude that RSM is worth using to predict the flow for this jet impingement case, despite the fact that the solution took longer to resolve.

3.2.5 Further Height-Based Analysis

Having determined the superiority of the Reynolds Stress Models method, RSM was then used in order to study the behavior of the flow, moving away from the plate surface and closer to the nozzle exit. In order to do so, lines were drawn during post processing the results on ANSYS Fluent, going upwards from the specimen line to the nozzle exit half a millimeter at a time. Then the Velocity Magnitude, Radial and Axial Velocities were drawn for each of these lines. The results, after erasing the lines where the flow did not change drastically in order to make the diagrams more readable, are shown in Figure5.

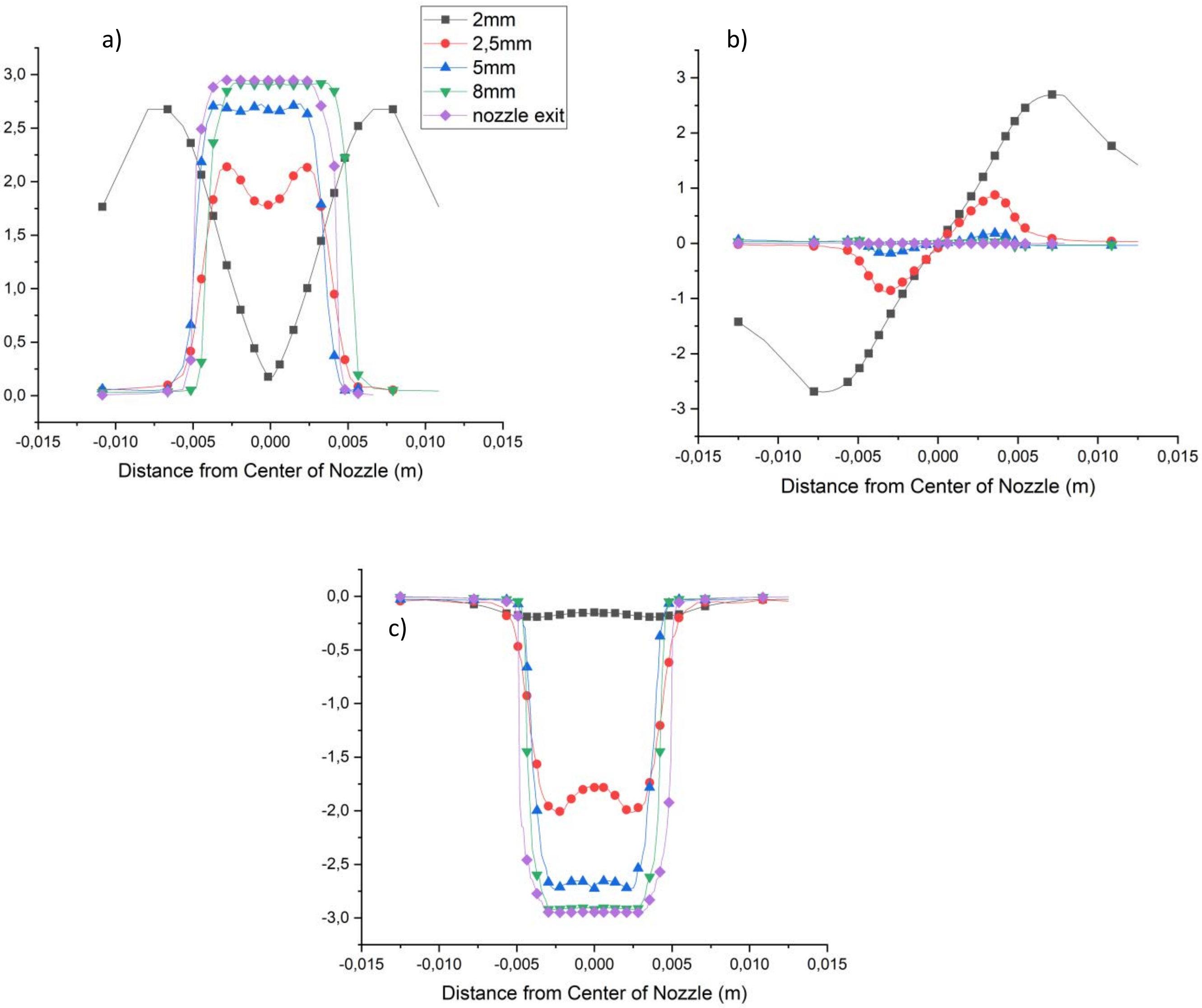

Figure 5: Results for the Velocity Magnitude (a), Radial Velocity (b) and Axial Velocity (c) at heights 2mm, 2.5mm, 5mm and 8mm above the plate

It is evident that Velocity gradients become less steep as we move on closer to the exit of the nozzle, solidifying our earlier choice to study the flow complexity and the models' ability to predict at heights closer to the specimen.

Chapter 4: **Multiphase Flows**

4.1 Introduction to Multiphase Flows

The term Multiphase Flow can be applied to any type of flow that consists of at least two phases, meaning the state of matter for each component (*solid, liquid or gas*) (13). The majority of flows found in any industrial process, are multiphase flows, making the phenomenon crucial to understand and accurately predict. It is also important to note that the term phase can sometimes have a wider meaning than just the physical state of matter, to include cases where particles of the same state can have such a difference in size that they must be treated as different phases, because they react differently to the same flow field (13).

4.2 Multiphase Flow Categories

4.2.1 Physical State Categorization

There are four basic categories of Multiphase Flows, based on the physical state of each flow component. These are the Gas-Liquid, Gas-Solid, Liquid-Solid and Three-Phase Flows (13) (14).

Examples of Gas-Liquid flows are found whenever encountering the movement of bubbles inside a liquid (*i.e. spray atomization in the combustion chambers of power generating plants or oil-gas flows*), or the movement of liquid droplets in a gas stream (*i.e. steam-water flows inside the pipes of a heat exchanger*) (14).

Gas-Solid flows most often describe the movement of solid particles suspended in a stream of gas. This is the type of flow we can see when encountering cyclones separators or the combustion of coal particles in fossil-fuel power stations. A unique case of Gas-Solid flow occurs when the particles have zero speed. Then the Gas-Solid flow is treated as a full gas flow through a porous material (14).

Liquid-Solid flows, or ‘’slurry flows’’, refer to the movement of solid particles inside a body of liquid. They are most commonly found in industrial transport applications when for example coals and ores are moved through a pipe in a slurry flow. Liquid-Solid flows are of great interest to this thesis as they will be the type of flows simulated later. (14)

Mixing any of the above flow types creates a new flow regime called a Three-Phase flow. For example there may be cases where bubbles are found inside a Liquid-Solid flow or even when Oil-gas flows may contain a significant quantity of water. Although methodologies are being developed to encounter Three-Phase flows, the most reliable method applied in the industry is to use a Three-Phase flow separator to process each phase separately (14).

4.2.2 Visual Categorization

Multiphase Flows are also usually categorized, based on the way the phases, their velocities and directions are visually spaced, into separated, mixed and dispersed flows (13) (14). Different combinations of these flow regimes can also co-exist an example being annular bubbly flow which contains separated and dispersed flow simultaneously.

Figure 6 (13) (14) shows a variety of different types of flows for horizontal and vertical pipes, while Figure 7 (13) is a flow map for two-phase horizontal pipe flows adjacent to the superficial gas and water velocities.

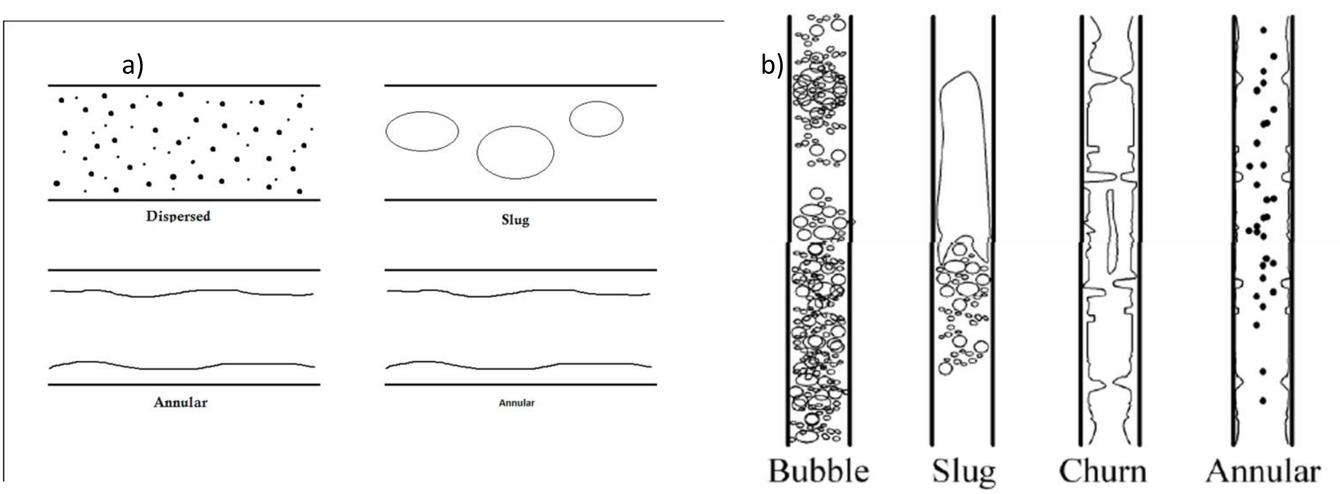

Figure 6: Different types of flow regimes in horizontal (a) and vertical (b) pipes (17)

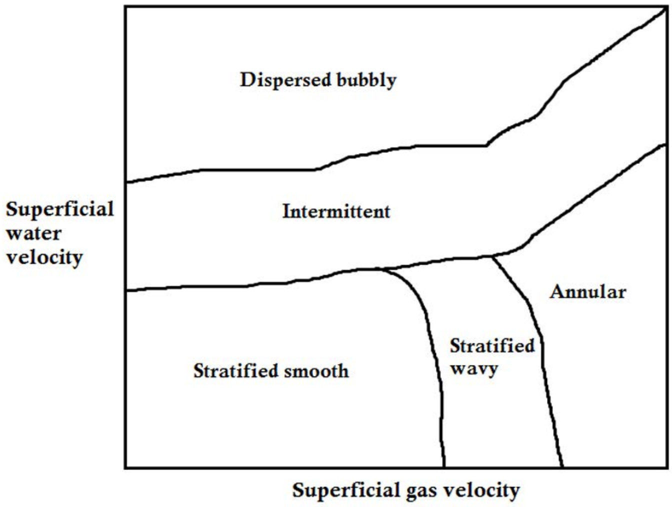

Figure 7: Flow map for two-phase horizontal pipe flows adjacent to the superficial gas and water velocities (17)

4.3 Modeling Approaches

Determining which modeling approach to choose when simulating a flow with multiple phases depends on the case geometry and physics as well as the computational power available. Different modeling approaches provide different levels of detail and precision in the expense of computing time.

4.3.1 Euler-Euler Method

The Euler-Euler method considers every phase to be a continuous medium and proceeds to solve the conservation equations for each phase separately (13). In order to couple between the phases, mutual pressure and interphase exchange coefficients are implemented (14). A variety of models have been created in order to calculate these coefficients. If individual particle movements are not of interest, the Euler-Euler approach can be used to simulate the overall motion of the sum of particles, even in cases where the flow is dispersed (13). However to allow such an averaging the density of the flow should be considerably high. A simplification of the Euler-Euler methodology is the mixture model, a model that implements mixture properties like velocity and viscosity in order to model both phases as an interpenetrating spectrum (13).

4.3.2 Euler-Lagrange Method

The Euler-Lagrange approach on the other hand proceeds to solve the motion equations for each individual particle of the dispersed phase (*both solid particles and gas bubbles*), while simultaneously solving the conservation equations for the continuous phase (13) (14). In contrast to the Euler-Euler method this approach is highly demanding in terms of computational time and power and is therefore usually preferred when dealing with flows of low particle density (13).

4.3.3 Volume of Fluid (VOF) Method

Another revision of the Euler-Euler model is the VOF (*Volume of Fluid*) method. The differencing factor to the Euler-Euler method is the fact that VOF does not allow for phase interpenetration. Instead, VOF uses a phase indicator function that takes the value of zero or one when only one phase exists within the control volume or the intermediate values when two phases coexist, indicating the volume fraction of each phase (13) (14).

4.4 Finite Volume Methods (FVM)

Regardless of the modelling approach chosen, directly solving all sets of equations that describe a flow is only realistic for very simple cases. In order to solve complex flows, Computational Fluid Dynamics (*CFD*) software apply numerical methods called FVM (*Finite Volume Method*), dividing the computational field into smaller, finite control volumes and solving the conservation equations for each cell. This creates a grid that ensures conservation in both cell and global scales (13) (14).

The two most spread versions of FVM are the Center Node Based and Vertex Based FVM. Both these methods solve the conservation equations for each control volume (13). However, in the Center Node Based FVM method information is stored in a node at the center of the cell and the values for the cell faces are calculated approximately using interpolation methods. Vertex Based FVM methods on the other hand, calculate and store values for the conservation equations in each cell corner and then the properties are administered to the corresponding control volumes (13).

Chapter 5: **CFD Model Validation-Mansouri Experiments**

In order to facilitate a comparison between the results of a two-dimensional and a three-dimensional study of the same jet impingement case, an ANSYS Fluent project was created based on the geometry examined by Amir Mansouri in his dissertation, entitled **'A COMBINED CFD-EXPERIMENTAL METHOD FOR DEVELOPING AN EROSION EQUATION FOR BOTH GAS-SAND AND LIQUID-SAND FLOWS'** (15)in both a 2D and a 3D environment. The CFD results for the Velocity Magnitude at the exit of the Nozzle, as well as the contours of Velocity Magnitude for the entire geometry, were then compared with the experimental measurements carried out by Mansouri (15).

5.1 Setup and Results

5.1.1 Geometry Setup

ANSYS Discovery was utilized to generate both the 2D and 3D geometries. A symmetrical approach was employed in the design of the array, with only half of it being constructed, in order to minimize the computational power requirements. The inlet diameter and the distance from the nozzle exit to the wall specimen were set at 7.6 and 12.7 mm, respectively, in order to align with the dimensions of the Mansouri experiments. The pipe length was set at 150 mm to ensure a fully developed flow before the nozzle exit, and the specimen at the bottom of the array was 37.5 mm wide.

5.1.2 Mesh Setup and Quality Metrics

ANSYS Meshing was used to create both the 2D and 3D meshes. Edge Sizing was done through the method of ‘’Number of Divisions’’, using the same divisions and bias factors in both cases, in order to ensure that both the 2D and the 3D meshes exhibited equivalent mesh density and that the results were not mesh-dependent. Face Meshing was also applied in order to generate a mapped mesh in the surfaces of interest. For the 3D case, a global sweep method was employed to obtain a fully orthogonal grid, and a minimum orthogonal quality of 50% was achieved for both cases.

5.1.3 ANSYS Fluent Setup

ANSYS Fluent was utilized for the configuration and resolution of the problem. Double Precision was enabled on the solver, and four Parallel Solver Processes were employed to enhance the precision of the results. In the physics section of the configuration, RSM was employed as the turbulence modelling approach, with water of 998.2 kg/m2 density and 0.001003 kg/m*s viscosity designated as the working fluid. The inlet boundary condition was set for velocity inlet, with a speed of 14m/s. The turbulence specification method used was Intensity (1%) and Hydraulic Diameter. Symmetry and No Slip conditions were applied for the fluid domain and the Walls, respectively, while Pressure Outlet boundary conditions were used on the outlets with an Absolute Gauge Pressure of 0 Pa. The SIMPLE scheme with Second Order Upwind Spatial Discretization was employed to couple pressure and velocity, with the residual absolute criteria set at 1e-06, thereby enhancing the quality of the results.

5.1.4 Results and Comparisons

The contours of Velocity Magnitude for the entire geometry using both the 2D and 3D environment are compared with the results from the Amir Mansouri dissertation in Figure 8, while the plots of the Velocity Magnitude at the exit of the nozzle are compared in the same plot with the experimental data provided also by Amir Mansouri in Figure 9.

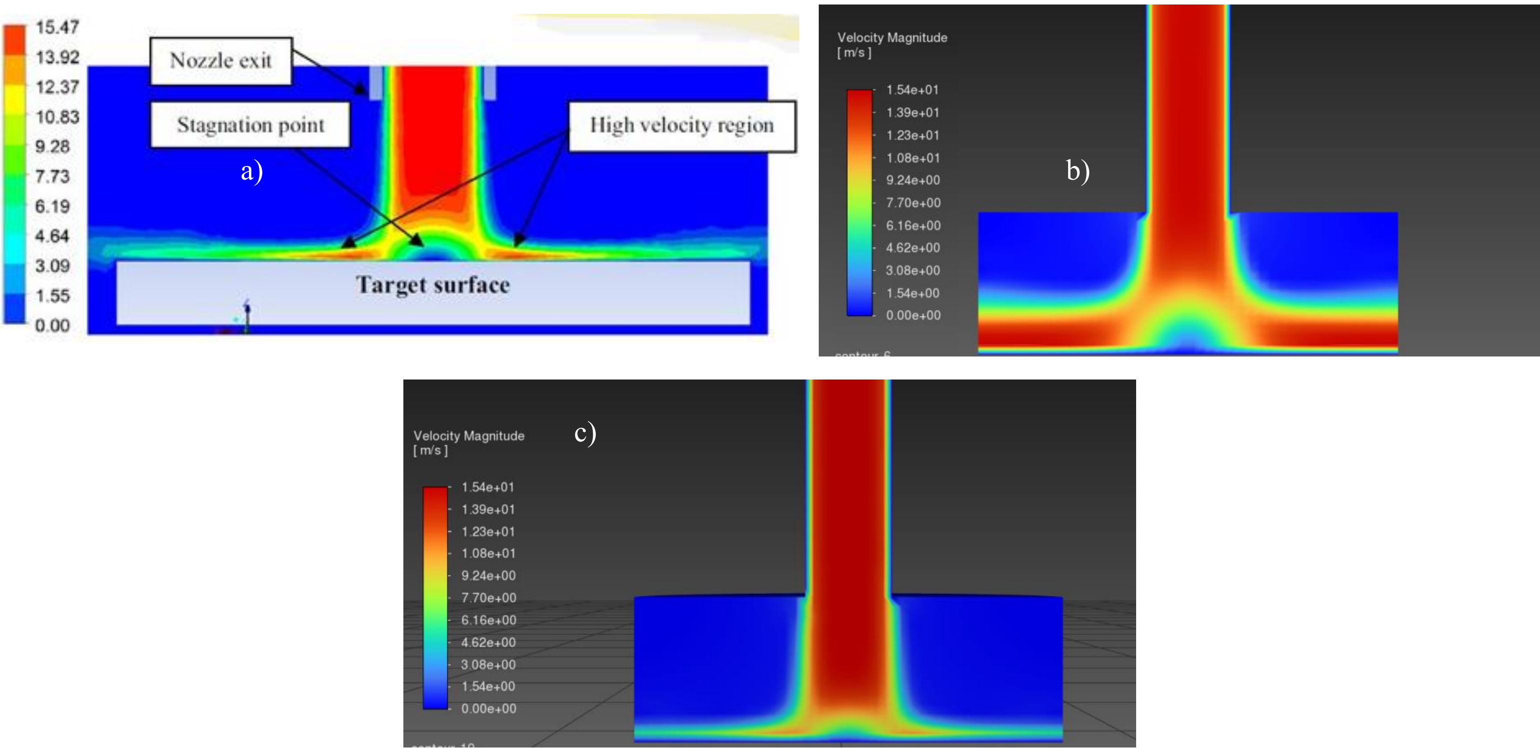

Figure 8: Contours of Velocity Magnitude provided by Mansouri (a), 2D CFD Simulation (b), 3D CFD Simulation (c)

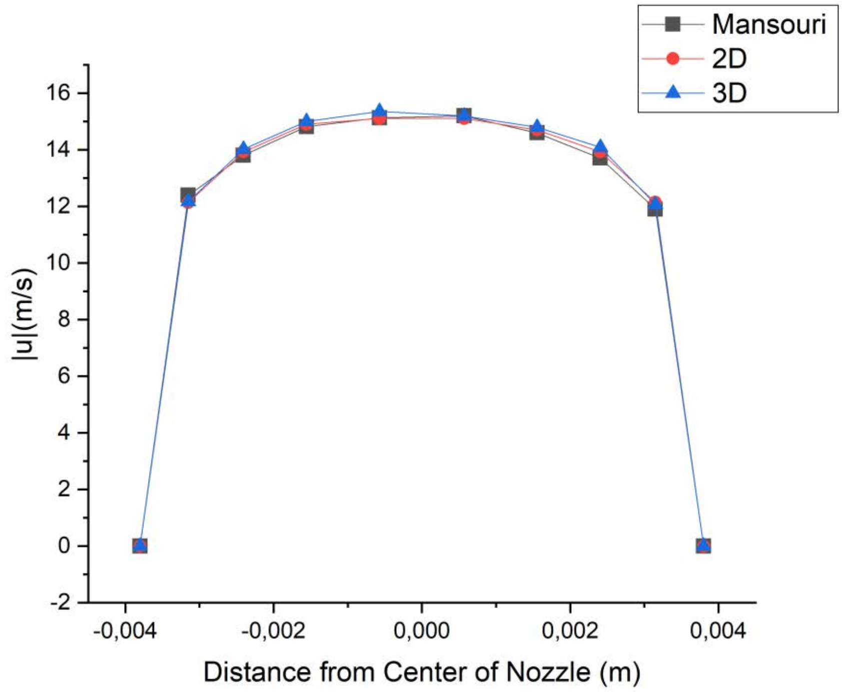

Figure 9: Velocity Magnitude at Nozzle Exit

The CFD models provided accurate results in both the 2D and 3D case when comparing the Velocity Magnitude at the nozzle exit. When it came to contouring the Velocity Magnitude for the entirety of the computational domain however, the 2D model proved incapable of providing sufficient accuracy in the results. The main differences were observed at the high velocity regions above and near the plate. In these regions the 2D case was unable to predict the turbulent intensity of the flow and it provided overestimations in the values of the Velocity Magnitude. This deficiency can be attributed to the fact that turbulence is a three-dimensional phenomenon, as evidenced by the 3D model's ability to accurately predict both the turbulent intensity and dissipation. The relief effect of having the third dimension should also be considered when trying to explain the differences between the 2D and 3D case. Based on these observations we can conclude that the 2D model can be used in occasions where only the absolute value of velocities is of interest and not the way that they are dissipated. In those cases of course the 2D model should be preferred as it provides highly accurate results, while demanding less computational power.

5.2 Erosion Simulations

5.2.1 Geometry and Mesh

Having determined the superiority of the 3D model in predicting the flow velocity and all its fluctuations, the 3D case was refined in order to be used in further simulations. Consequently, a quarter of the geometry was redesigned in ANSYS Discovery, leveraging the symmetry of the results at the sides of the array to minimize the calculations necessary to resolve the problem.

Similarly to the original 3D Mesh, Face Meshing and Sweep Methods were again used in order to create a mapped orthogonal mesh. In this case however sizing was done using the Body Sizing Method of Sphere of Influence in order to coarsen the mesh in the areas of interest (*i.e. close above the specimen and on the specimen surface*).To this end, a 5 mm radius sphere was positioned at the center of the specimen, with the dimensions of all elements within the sphere's influence modified to 0.1 mm.

5.2.2 Discrete Phase Model (DPM) and User Defined Function Setup (UDF)

To measure the erosion rate on the plate’s surface Discrete Phase Model (DPM)was enabled in ANSYS Fluent models tab. Interactions with the continuous phase and erosion physical models were enabled and a new injection was setup from the inlet surface. The parameters of the injection were set up in order to match the conditions of the submerged jet impingement erosion measurements carried out by Mansouri. A Rosin-Ramier Diameter was picked with a minimum particle diameter of 53 μm, a mean diameter of 300 μm and a maximum diameter of 710 μm, with 14 in-between values. The mass flow rate of the particles was set at 0.004 kg/s and the particle density was 2650 kg/m^3. Calculations were carried out with DPM iterations happening for every 10 solution iterations.

To plot for the actual erosion depth on the specimen’s surface a new User Defined Function (*UDF*) was created to turn the results of erosion rate into erosion depth measurements. The Finnie erosion model was used in order to calculate the erosion rate and then turned into erosion depth using the following formulation.

$$erosion\ depth(mm) = \frac{erosion\ rate * time}{density * 1000}$$

The duration of the test was 6 hours and the density of the specimen’s material was 7850 kg/m^2.

5.2.3 DPM-DEM Literature and ANSYS Settings

Discrete Phase Model (*DPM*) is a Lagrangian model that adopts the Euler-Lagrange approach to solve Multiphase Flows. As mentioned on the chapter about Multiphase Flow modeling this approach solves the motion equations for each individual particle while simultaneously resolving the continuity equations for the liquid flow. The complexity of the method made it suitable for solving flows with low particle concentration like the ones modeled in this thesis. However, it should be noted that DPM is also suitable for high mass loading cases. During the simulation of the fluid flow, particle trajectories are calculated at specified intervals (*flow iterations*) so computational cost and time in cases with high particle concentration could be reduced by increasing the gap between each DPM iteration. In ANSYS Fluent the choice between one or two way coupling is also available when enabling or disabling the *interaction with continuous phase* option.

Discrete Element Method (*DEM*) is a computational method that combines Newton Laws and Contact Mechanics to individually calculate inter-particle forces acting on the flow, by the implementation of contact detection algorithms (19). Rotational accelerations and shape dynamics are also considered when using DEM to solve a multiphase flow case. DEM's precision and complexity makes it more suitable for simulations at molecular levels or cases where structure and mechanical behavior of the mixture is of interest (20).

In the cases studied two-way coupling DPM was used as the way to set up and simulate the multiphase flow. ANSYS Fluent allows us to control which Physical Models will be taken into consideration when simulating the multiphase flow.

Erosion/Accretion calculates the erosion rate on stationary walls in the geometry. As erosion depth on the impinged plate surface was the point of interest of the study, Erosion/Accretion was the first Physical Model enabled.

Virtual Mass and Pressure Gradient Forces were enabled and expected to influence the results as they are mostly applied in cases where the phase density ratio is low.

Saffman Lift Force was also enabled but didn't have significant impact on the final results, as expected by the fact this force mostly acts on sub-micron particles.

Two-Way Turbulence coupling was enabled to account for the turbulence eddies in the flow caused by damping effects.

Particle Radiation Interactions, Thermophoretic Forces, Pressure Dependent Boiling, Stochastic Collisions and Breakups are also available but were of no interest, thus not enabled during the simulations.

5.2.4 Results and Comparisons

The results of the CFD simulations compared to the measurements done by Mansouri are shown on Figure 10.

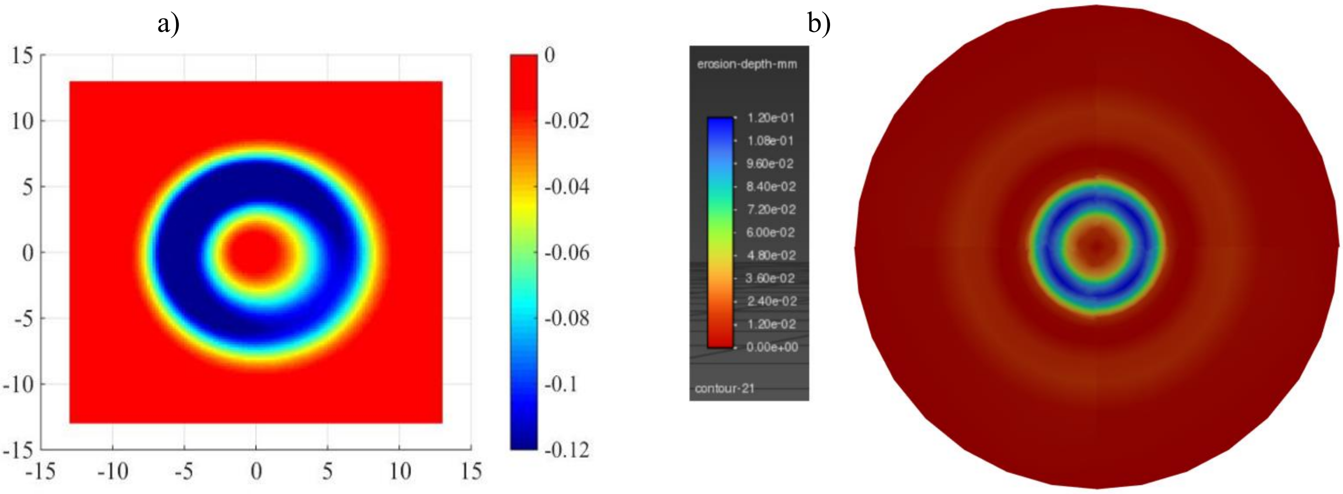

Figure 10: Contours of Erosion Depth in mm, as measured by the Mansouri tests (a) and CFD Simulation (b)

It is observed that the CFD Model did well to predict both the erosion pattern and the erosion depth after 6 hours of testing. Given the fact that most erosion studies' practical point of interest is to identify the areas where erosion will be more intense in order to expect an upcoming failure, this domain and model combination is adequate enough to provide the needed results.

.5.3 Erosion Depth to Inlet Velocity Study

On top of that a study for the development of the erosion depth on the centerline of the specimen was carried out using the CFD Models and the UDF, as the inlet velocities for both the liquid and the particles were progressively reduced. Results for the erosion depth on the specimen centerline at 12, 8, 5 and 3 m/s are shown in Figure 12.

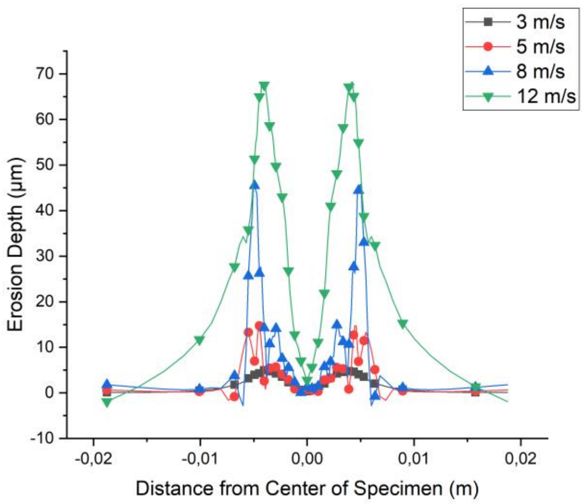

Figure 11: Erosion Depth on the centerline of the specimen at different inlet velocities.

As expected an increase to the Inlet Velocity resulted in an increase on Erosion depth on the plate's centerline. It is worth noting that the differences in Erosion depth were smaller as Inlet Velocities reduced.

5.3 Measuring the Length of Erosion Zones

A comparison was made of the lengths of each erosion zone, as measured by the CFD results and the experimental data provided by Mansouri, using the above quarter geometry and settings. Following a series of simulation trials, the Finnie erosion model emerged as the closest match in terms of predicting the scale of erosion depth when compared to the results obtained by Mansouri, with the McLaury model also showing promising results. The erosion depth scale measurements for both the experimental data and the CFD results are shown in Figure 13.

a)

b)

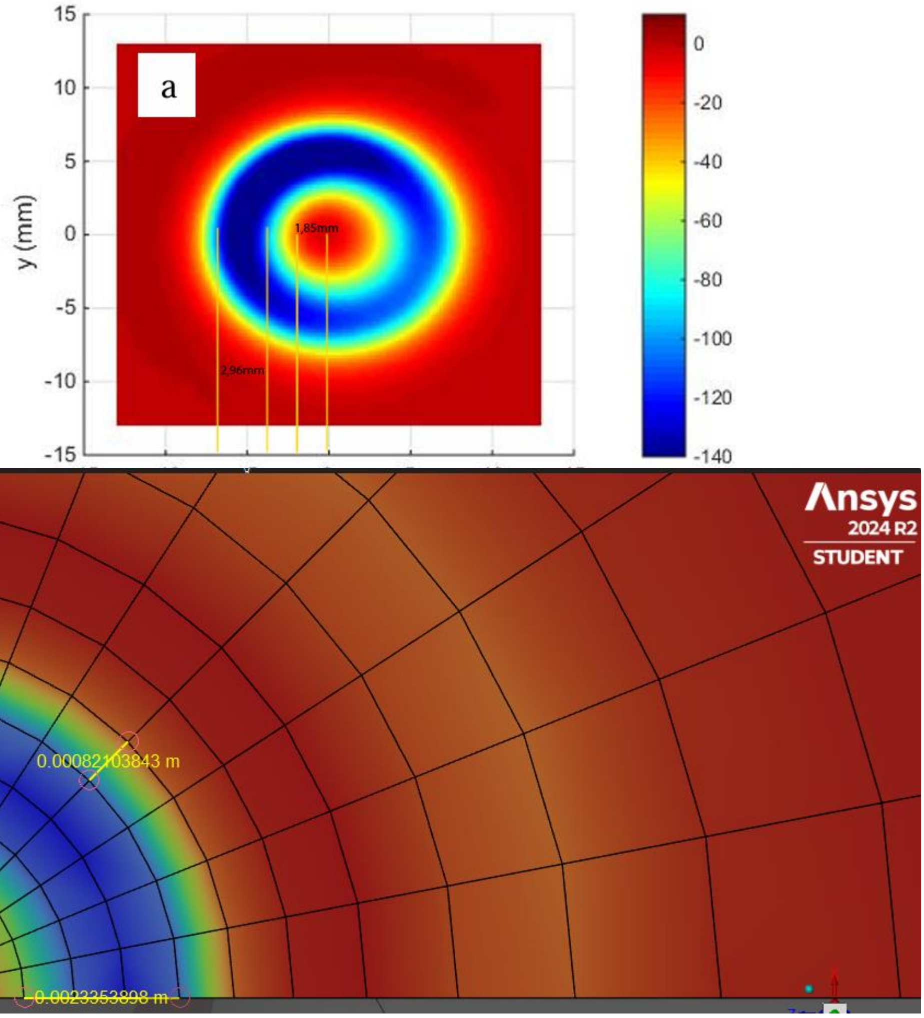

Figure 12: Length of erosion depth regions as given by a) Mansouri experiments b) CFD simulations

The radius of the low-erosion region in proximity to the stagnation point at the center of the plate can be estimated by plotting vertical lines on the experimental results, which yield an approximate radius of 2 mm. After measuring the node spacing of the CFD results using the tool provided by ANSYS Fluent in post-processing, the radius of the erosion depth came to 1.52 mm. Other erosion models either didn't predict the erosion zone lengths as well (*i.e. the Oka erosion model*) or didn't even correctly simulate the pattern (*i.e. the generic erosion model*).

5.4 Analysis using Symmetrical Geometries

Quarter Symmetry proved to be adequate enough to predict the erosion pattern and erosion depth on a horizontal plate. When considering the case of an inclined plate though, quarter symmetry doesn't apply, since the geometry stops being symmetrical on quarter level. With this in mind and in the spirit of trying to improve convergence time and computational power needed, another study was carried out to evaluate the ability of symmetrically designed geometries to generate accurate flow results. For this cause the same geometry was designed five times. The first one included the full geometry (360^o of it) and was used as a reference point. The other four designs utilized the symmetrical nature of the problem, allowing us to design half of the geometry (180^o of it) and three cases where 90^o, 30^o and 15^0 splines were designed. Free surfaces were treated by applying the symmetry boundary conditions so the solver only had to solve the ratios of the geometry designed each time. Velocity Magnitude Contours as well as Nozzle Exit Graphs were compared. Velocity Fields were accurate no matter the geometry used when compared to experimental measurements however when studying the Nozzle Exit Velocity Graphs there was a clear connection between percentage of geometry simulated and result accuracy. These results are shown in figures 14 and 15.

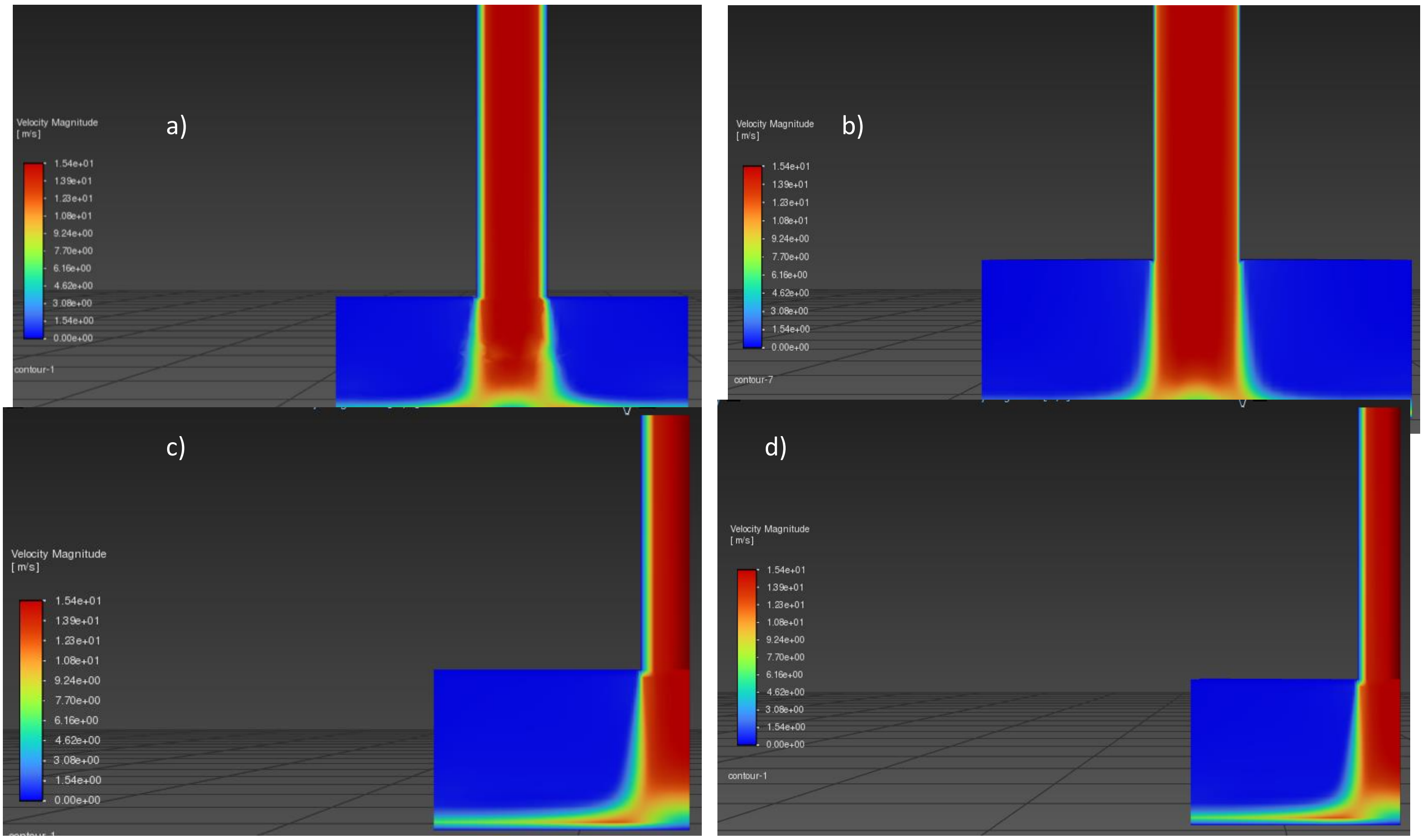

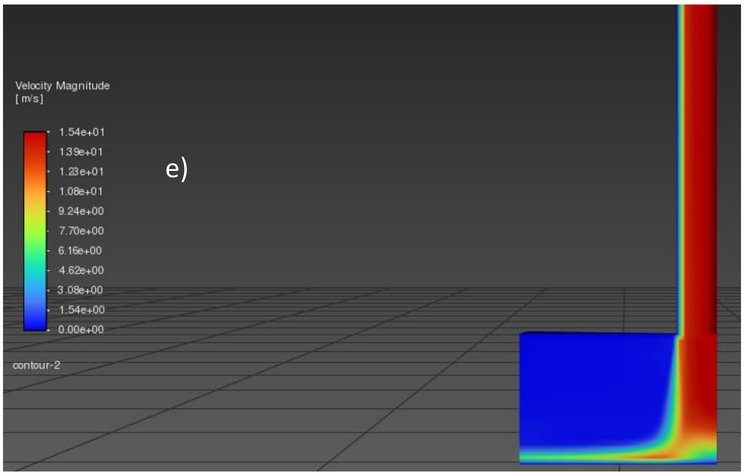

Figure 13: Velocity Magnitude Contours of a) Full Geometry b) 180 Degree Geometry c) 45 Degree Geometry d) 30 Degree Geometry and e) 15 Degree Geometry

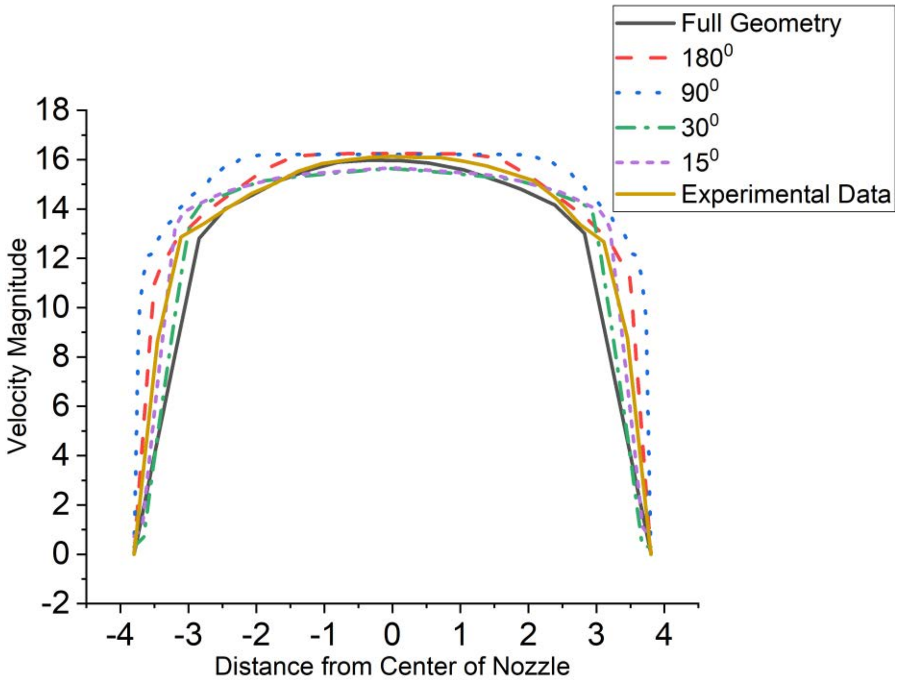

Figure 14: Nozzle Exit Velocity Magnitude using different percentages of the Full Geometry

All geometries performed adequately in simulating the Velocity Magnitude Contours, as there were no notable discrepancies when compared to either the previously designed contours or those derived from Mansouri's experimental measurements. However, upon examining the Nozzle Exit Velocities, variations in the Velocity Magnitude became apparent as more of the geometry was resolved symmetrically. It was observed that the largest deviations occurred further away from the stagnation point, a region where erosion was either negligible or entirely absent according to prior analyses.

Given this, it is reasonable and safe to adopt the 180° geometry for the simulations. This particular geometry applies the symmetry boundary condition solely along the z-axis, which makes it suitable not only for flat plates but also for inclined plate configurations. Furthermore, it maintains a strong agreement with the experimental data, ensuring that accurate and reliable end results can be expected in the subsequent erosion and flow analysis.

Chapter 6: **Erosion Simulation on Inclined Plates**

Having established the preferred viscous, mesh, fluid settings and erosion rate models for this multiphase jet impingement case it is now time to draw some additional geometries designed to simulate the erosion patterns for plates at an angle.

6.1 Designing the Geometries

In order to achieve this, it was necessary to redesign the 180-degree geometry for each individual case. This was not only because, as was previously demonstrated, this geometry provides accurate results while maintaining a low computational cost, but also because the quarter geometry would no longer be applicable. The reason for this is that angled plates make the geometry asymmetrical at quarter level.

In the following simulations, geometries including the sides and the bottom part of the computational domain underneath the plate were designed in order to account for the asymmetries created by the inclined nature of the case. To achieve an easily meshed geometry tilting the pipe and keeping the plate horizontal was preferred. The plate was designed to be cylindrical a design that enable it to be axissymetricaly swept using wedges and provided a mesh that was persistent with the simulations that previously gave accurate results. Splitting the geometries in 7 different bodies (*as shown in Figure16*) to ensure every single one of them is sweepable, proved to be the way to create the meshes that exhibited optimal orthogonal quality.

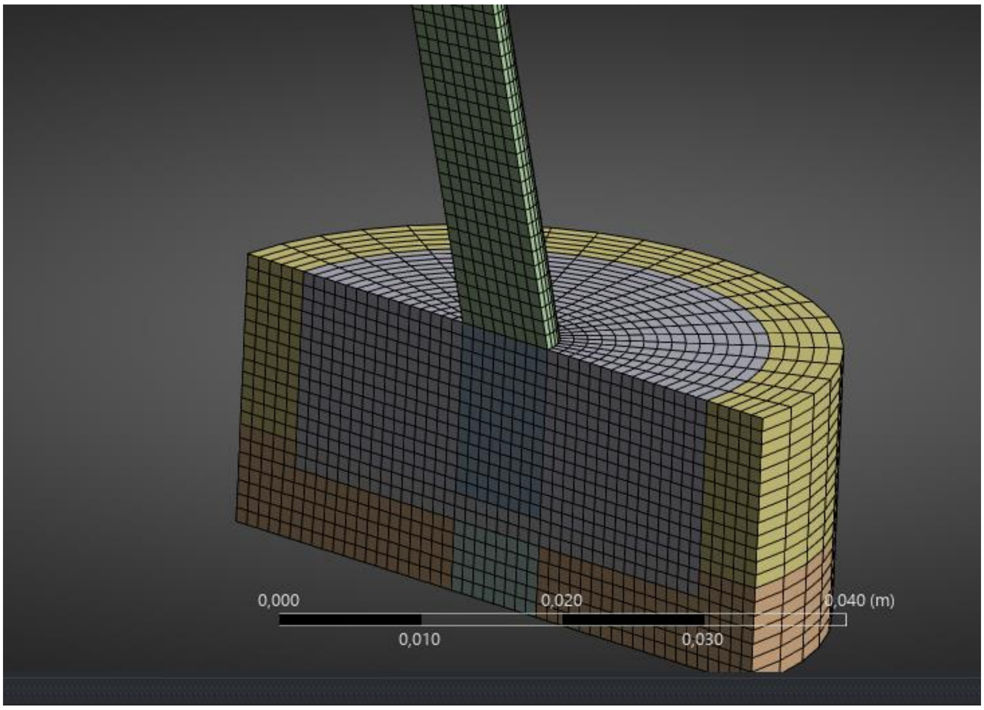

Figure 15: Geometry and Mesh for the 15 degree inclined pipe case

Different colors in Figure 1 represent different bodies in the geometry. Splitting the geometries in this way ensured every single body had an identical start and finish surface so a sweep method could be used on it. Sweeping every single body produced a mesh that was consistent and provided high orthogonal quality throughout the whole geometry.

6.2 Mesh Setup and Quality Metric Graphs

Figure 17 shows the mesh setup and metrics of orthogonal quality, for the different geometries created during these simulations.

a)

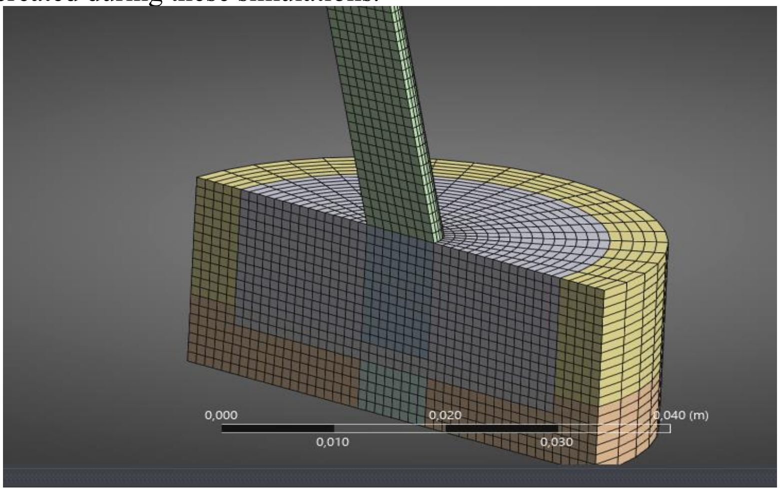

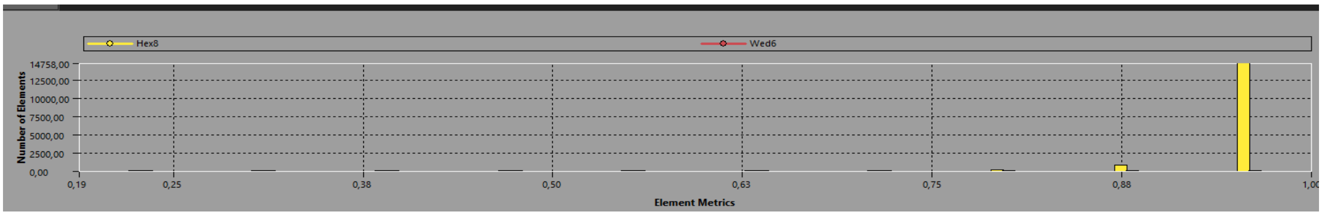

b)

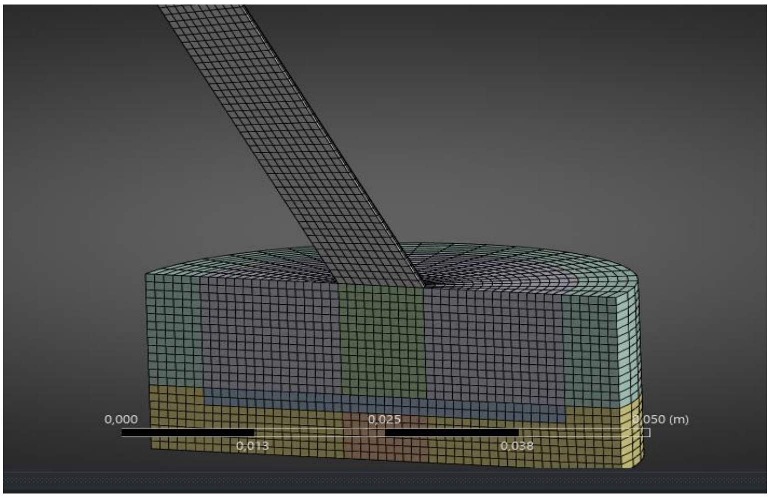

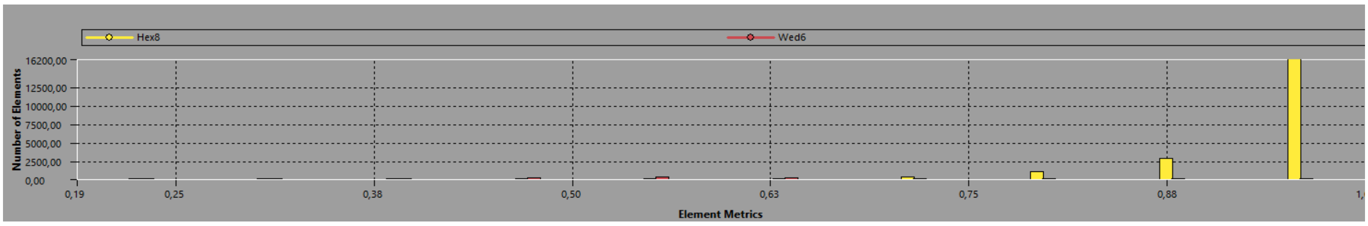

c)

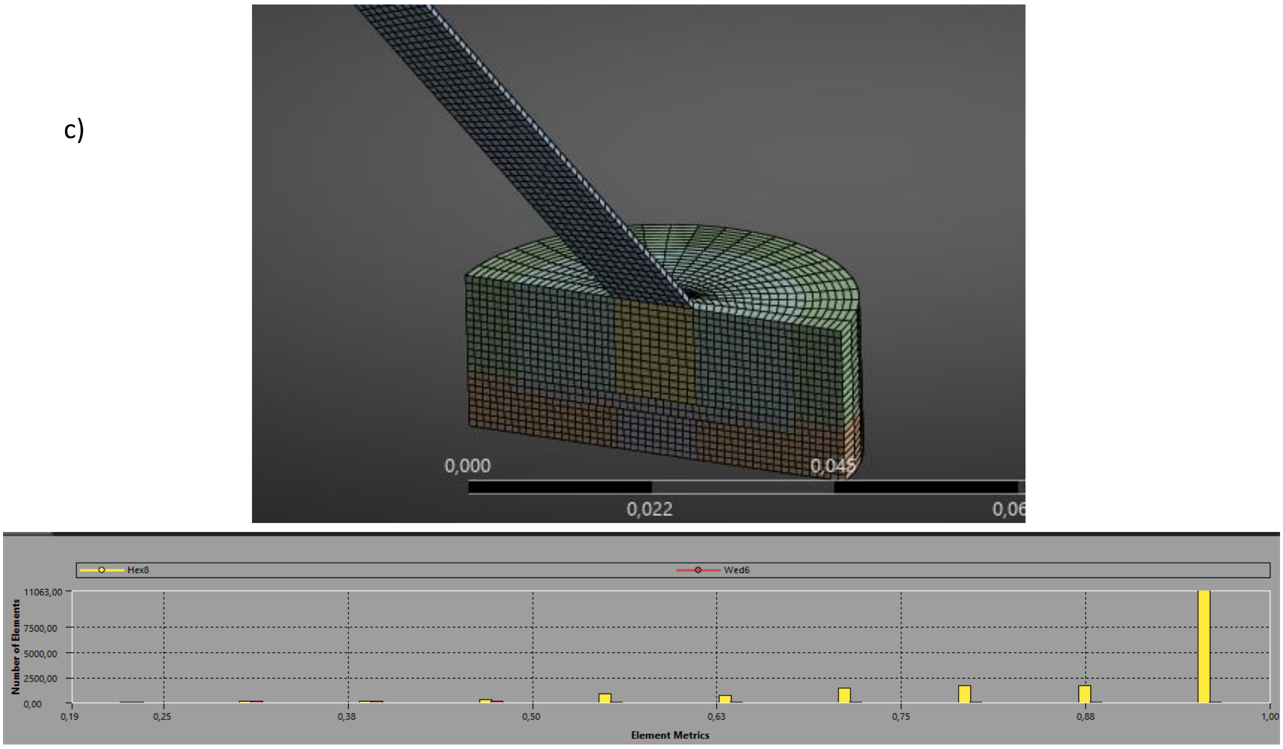

Figure 16: Mesh and Metrics of Orthogonal Quality for inclinations of a) 15 degrees b) 30 degrees and c) 45 degrees

ANSYS considers any element with an orthogonal quality metric greater than 0.1 as a high quality element that is expected to produce accurate results. The metrics shown in Figure 2 show that the elements of all cases have a minimum orthogonal quality of at least 0.22, with the largest number of elements having an orthogonal quality close to 100%. On the metrics tab there are 2 types of elements, Hex8 meaning a hexagonal element with 8 nodes and Wed6 meaning an element made closer to the geometry of a prism, made up of 2 wedges and having 6 nodes. Figure 18 shows the mesh of the impinged plate, which was the same for all cases.

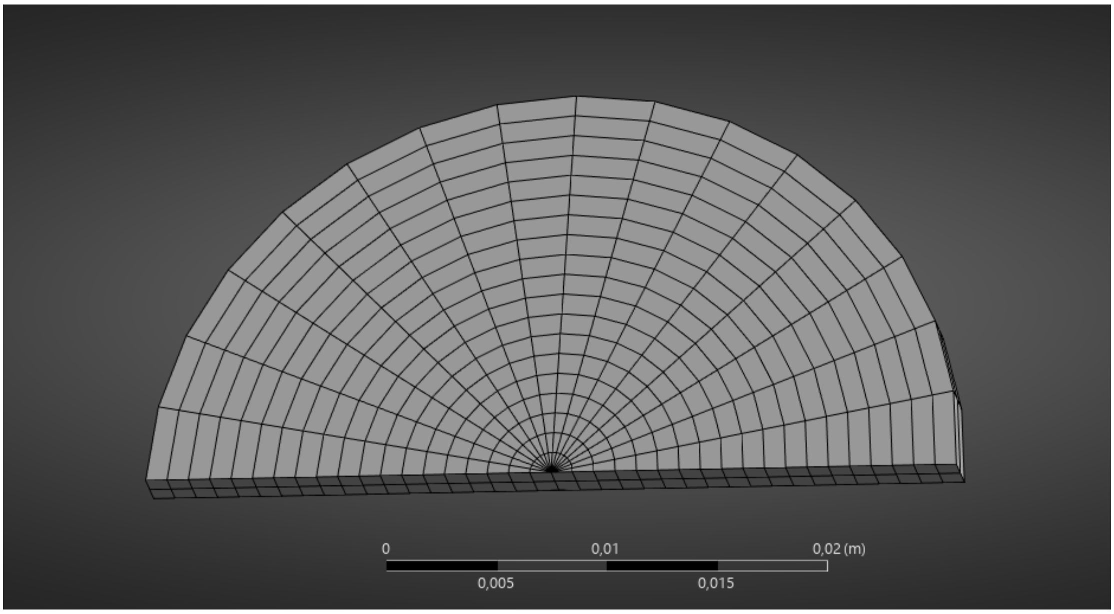

Figure 17: Plate Mesh used for all the simulations

As mentioned above, the cylindrical plate allowed the mesh to be axisymmetric and the sweeper to use the wedge method, giving us the best mesh for such a case. The sweep method was also applied to the rest of the bodies with the element size set to 1mm to meet the DPM requirement that the element size must be larger than the particle diameter.

6.3 Solution Setup and Single Phase Velocity Magnitude Contours

Single-phase simulations for the liquid-water phase at pipe-plate angles of 15, 30 and 45 degrees were initially carried out in ANSYS Fluent. RSM was used to simulate the flow in all inclined plate cases. RSM was previously determined to be the model that most accurately predicts turbulence behaviours. Inclined plate cases have by their nature more oscillations due to their more adverse velocity gradients creating more turbulence, thus making RSM a must use model. The contours of Velocity Magnitude for the cases of 15, 30 and 45 degrees plate angle are show in Figure19.

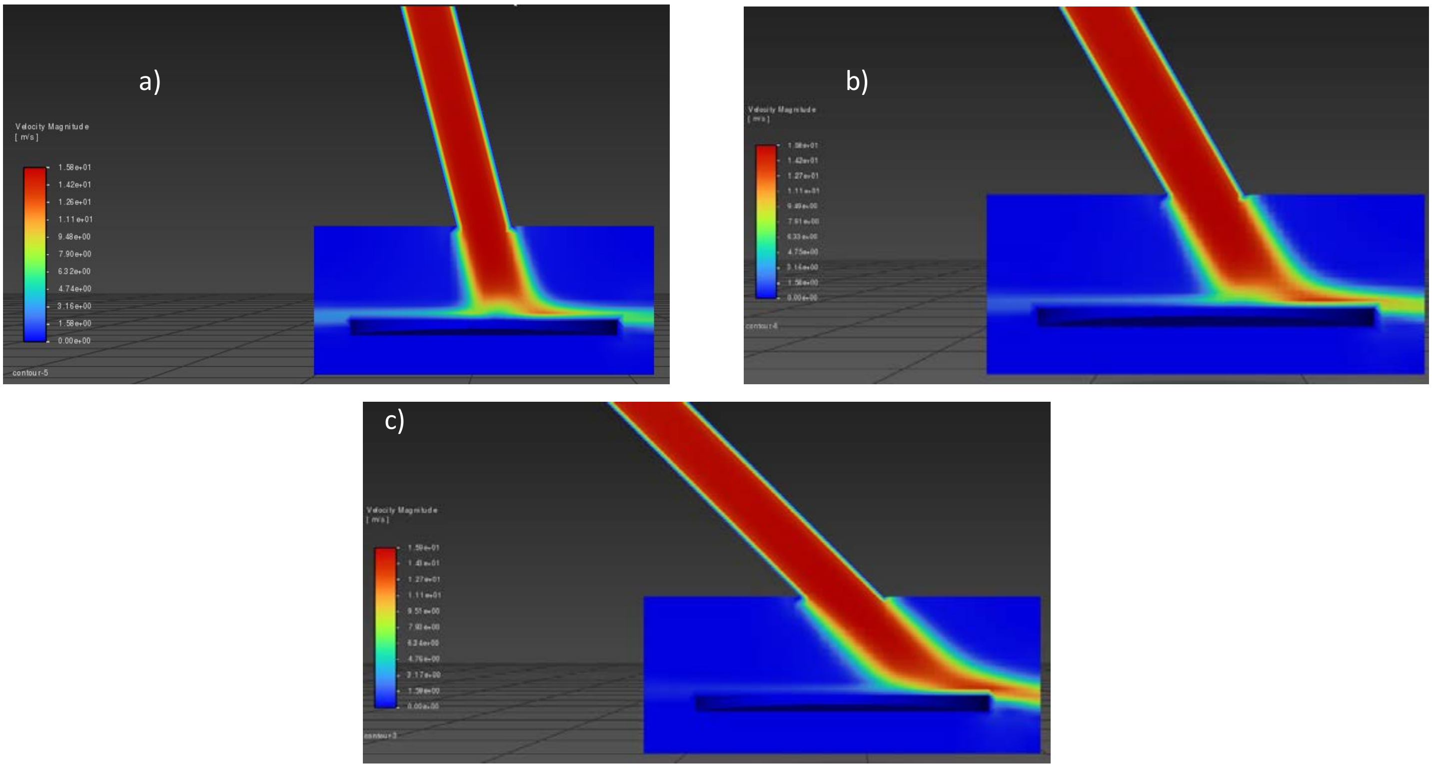

Figure 18: Contours of Velocity Magnitude for Pipe-Plate angles of a) 15 Degrees b) 30 Degrees and c) 45 Degrees

6.4 Erosion on Inclined Plate Surfaces

In ANSYS Fluent the DPM for the Erosion/Accretion simulation was set in the same way it were set before, when solving for the horizontal pipe-plate case, to match the conditions of the Mansouri experiments. In order to simulate the non-uniform way in which the particles entered the pipe through the inlet, the stagger position feature was enabled when setting the injection, with a stagger radius of 1mm. DPM iterations were conducted every second flow iteration. Results for the erosion depth of the plate surface at 15 and 45 degree angles are being compared to the measurements done by Mansouri at Figure 20, while the CFD results for the erosion rate at a 30 degree angle are presented on Figure 21.

a)

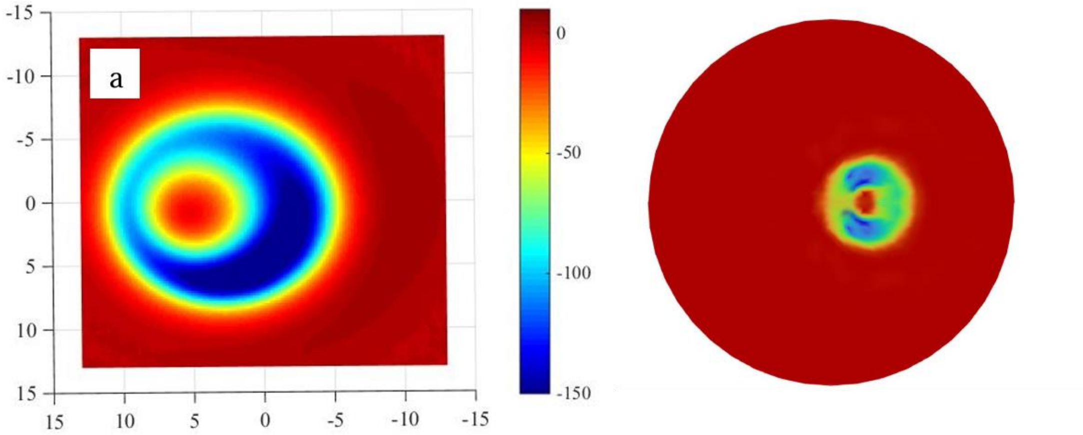

b)

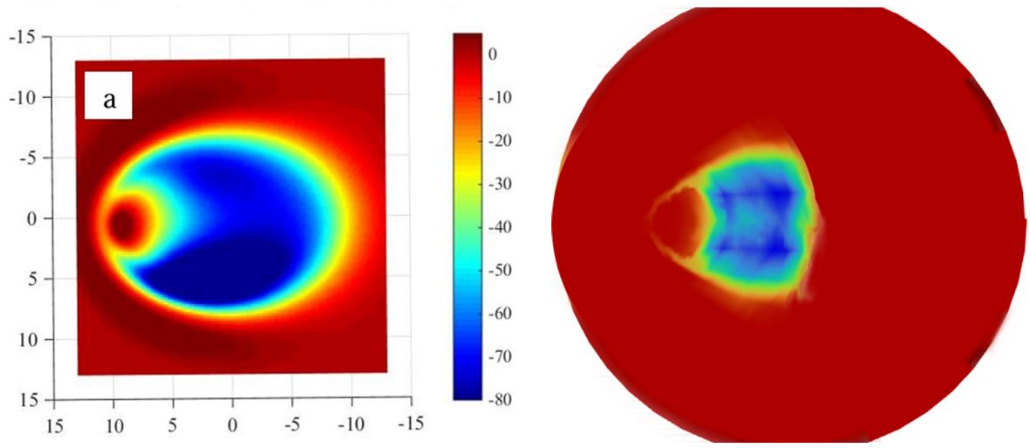

Figure 19: Erosion Depth on the Surface of the Plate as measured by the Mansouri experiments (left) and CFD simulations (right) for plate angles of a) 15 degrees and b) 45 degrees

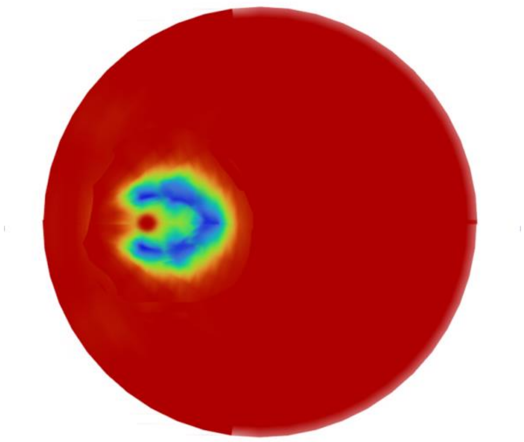

Figure 20: CFD Results for Plate Surface Erosion Depth at a 30 Degree angle

Erosion patterns and depth were closely matched when compared to the experimental measurement near the stagnation point for most cases. However, as the distance from the center of the plate is increased, the accuracy of this comparison is found to decrease, due to the increasingly complex and turbulent nature of the flow. The reason behind that could possibly be due to the element size of 1mm being excessively large. It has to be reminded that element size was set at 1mm in order to be comfortably larger than any particles released into the flow, which is a basic premise of multiphase CFD simulations (*maximum particle size for this experiment was 0,71 mm*). This leads to the program utilizing interpolation algorithms in order to predict the results between the nodes, possibly creating the discrepancies observed. This theory is further substantiated when measuring the erosion zones in the horizontal plate case, where most transitions occurred at scales smaller than 1mm.

6.5 Refined Mesh Simulations

Changing the element size near the plate would lead to inflations also making the elements of the domain smaller than 1mm, causing problems in simulating the flow. However, having devised the geometry in the way presented earlier not only allows for a fine mesh but also gives us the option of applying a body sizing method only to the plate. As the plate is a separate body the element size of the rest of the geometry would remain unchanged satisfying the restrictions we were facing earlier, while simultaneously allowing for more accurate erosion results on the plate's surface. The new refined mesh of the plate, after setting the element size at 10^{-5} meters can be observed in Figure 7.

Changing the element size only for the plate didn't increase the simulation time needed to resolve the flow, but DPM iterations took longer as it was expected. The refined results of erosion depth at plate angles of 15^o, 30^o and 45^o are shown in Figure 8.

Another important parameter in having smoother and more accurate results when simulating the erosion depth and patterns for the inclined plate cases was the density of the inlet mesh. Here refining the element sizes for values smaller than the particles' diameters was also possible without leading to any inconsistences caused by breaching the basic DPM principles. In order to only coarsen the mesh on the inlet surface and keep the elements for the rest of the pipe untouched we had to change the body method for the pipe from sweep to a hex dominant method. Then, surface sizing with an element size of 1e-04 was applied only for the inlet surface. This led to inflations lowering the overall orthogonal quality of the elements, providing however smoother and more accurate results for erosion depth, without influencing the overall flow accuracy.

Side to side comparison of the initial and refined plate mesh as well as the refined inlet mesh are shown in Figure 22.

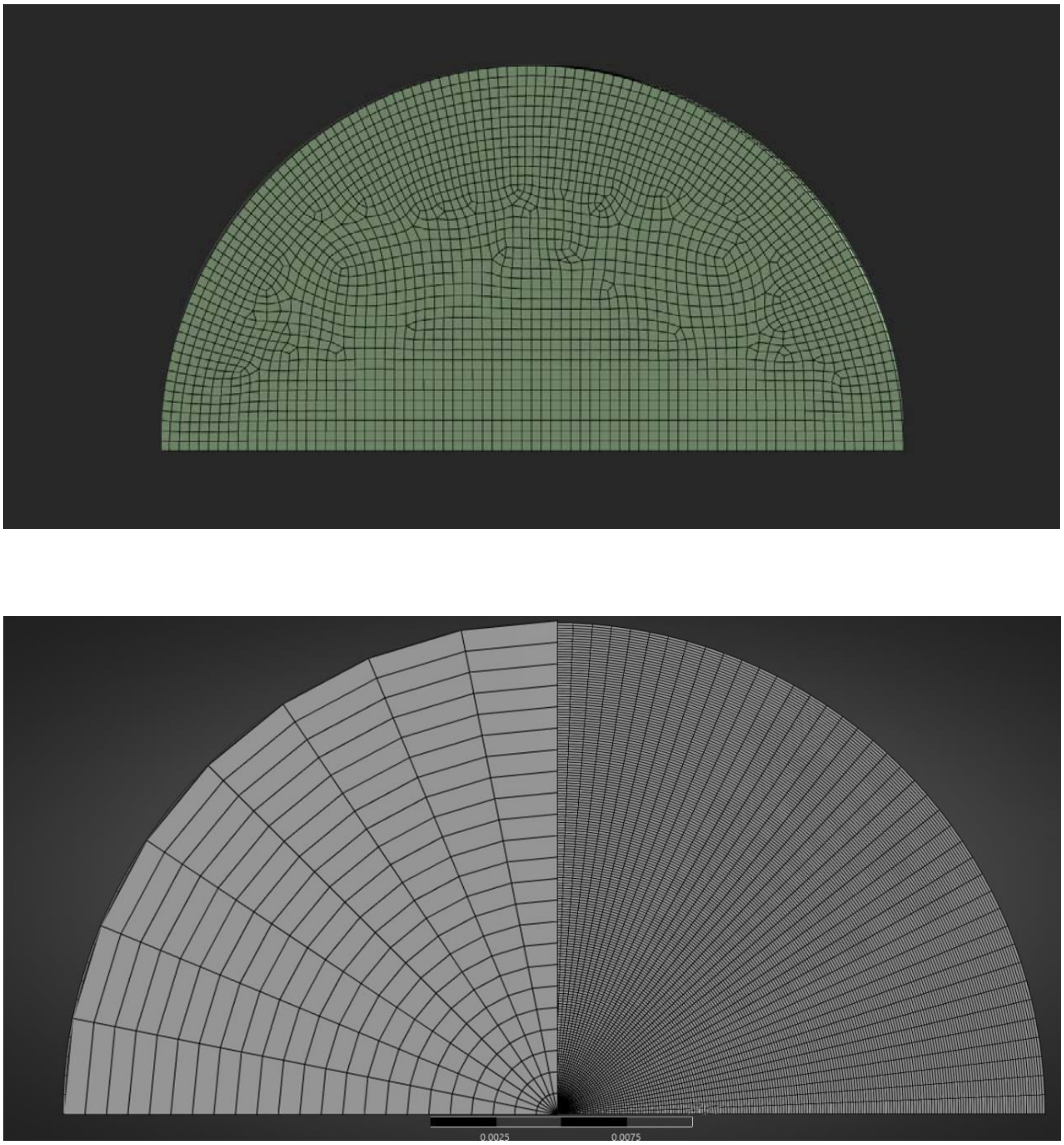

Figure 21: Refined Inlet Mesh (Upper Image) and Side by Side comparison of initial and refined plate surface mesh

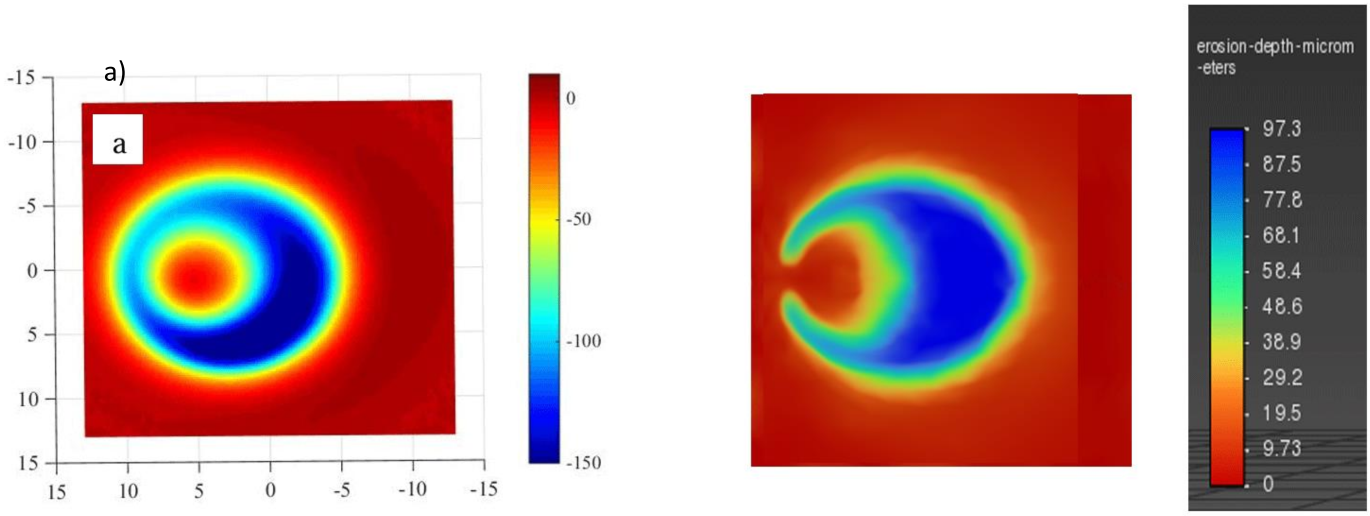

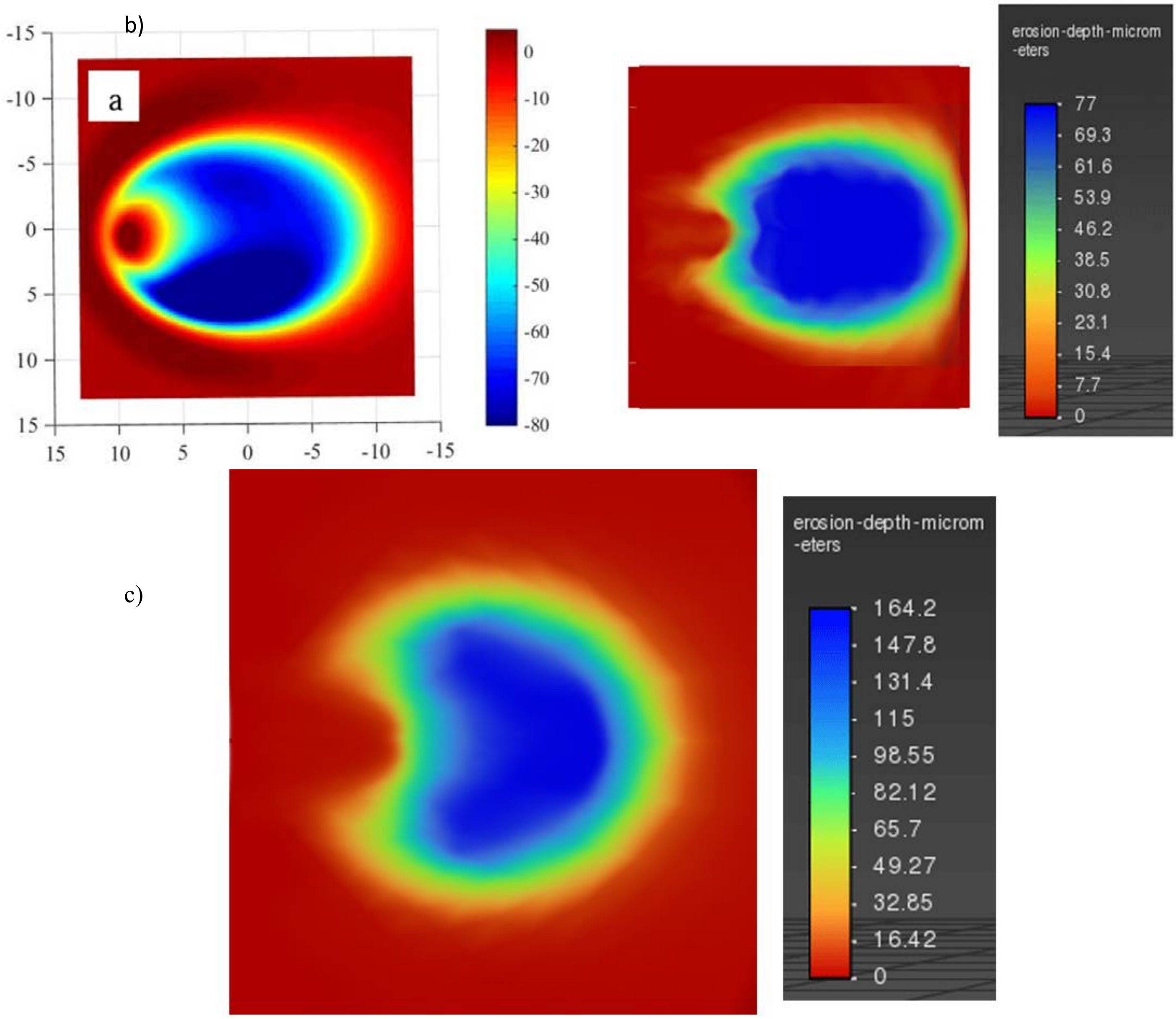

Figure 22: Erosion Depth as Measured by Mansouri's Experiments (Left) and CFD Simulations (Right) for plate angles of a) 15o b) 45o and c)CFD Simulation of Erosion Depth at 30o Plate angle

The application of the refined mesh resulted in enhanced erosion pattern prediction and more precise depiction of the erosion zone separations (*As seen in figure 23*). Different Erosion Depth scales are now shown for the CFD results as the denser mesh captured results and fluctuations in Erosion Depth that were not observed before, when using the same scale for both experimental measurements and CFD. These results clearly showcase the need of better mesh resolution when attempting to simulate the Erosion Depth especially on inclined plate cases where flows are much more complex and turbulence influences results on a larger degree.

Chapter 7: **Conclusions – Future Work**

The present thesis examines a variety of different single-phase and multiphase jet impingement flows, undertaking a direct comparison of the CFD results with those that have been experimentally validated. In the context of single-phase liquid flow, a range of turbulence modelling approaches have been adopted to simulate the behavior of the impinging jet. However, these approaches have encountered challenges in predicting the turbulent flow in the region near the stagnation point at the center of the impinged plate. Specifically, among the models examined (k-ω SST, RNG k-ε, RNGE k-ε with Enhanced Wall Treatment and RSM), the turbulence modelling approach that yielded the most accurate results was RSM. It was also noted that the implementation of Enhanced Wall Treatment and Production Limiters algorithms was justified, despite the associated increase in computational demands, as a result of the enhancement in the precision of the outcomes. RSM was then utilized to simulate and compare the velocity magnitudes, the axial and radial velocities at various heights above the impinged plate. This provided a clear picture of how the flow behaved and developed. The subsequent Multiphase Flow was set to match the conditions of the experimentally validated results available, using the DPM feature of ANSYS Fluent. The initial simulations were conducted with the objective of determining whether a 2D geometry would be adequate for simulating the multiphase flow. The conclusion drawn from these simulations was that the 2D geometry was inadequate in predicting the turbulence intensity of the flow. This indicated that the 3D case was necessary for a more accurate prediction. In addition, comparisons were made that exploited the symmetrical nature of the problem. Different portions of the geometry were simulated on each occasion. It was concluded that simulating 180° of the geometry was sufficient to produce accurate results and reduce computational cost. In view of these results, simulations were conducted to predict the erosion depths and patterns of a horizontal jet impingement case, as well as inclined plate cases. In the course of these simulations, a significant limitation of the methodology was identified with regard to the fundamental principle of DPM and the computational power available. It is evident that the quality of the results, particularly in relation to the angled plate cases, requires enhancement. The refinements made to the specimen and inlet surfaces were outlined in the thesis, and the results for erosion depth and patterns were evidently enhanced.

Moving on, using the way the geometries were separated into bodies presented in this thesis, further refinements could be done by inflating the domain even further, provided a more powerful computer is available. Other ways to overcome the existing limitations could be utilizing a hybrid resolved-unresolved CFD DEM approach, an AMR (*Adaptive Mesh Refinement*) method around the perimeter of the particles or further simulations examining the importance of lubrication effects on erosion patterns.

REFERENCES

1. **Mendi Chen, Lei Tan.** An improved method combined modified drag model and modified erosion model based on LES for solid-liquid multiphase flow and erosion with application in a 90 degree elbow. *State Key Laboratory of Hydroscience and Engineering, Department of Energy and Power Engineering, Tsinghua University, Beijing, 100084, China.* 2023.

2. **Rached Ben-Mansour *, Hassan M. Badr, Abdulrazaq A. Araoye and Ihsan Ul Haq Toor.** Computational Analysis of Water-Submerged Jet Erosion. *Mechanical Engineering Department, King Fahd University of Petroleum and Minerals,Dhahran 31261, Saudi Arabia.* 2021.

3. **Chuan Wanga, Xikun Wanga, Weidong Shia, Weigang Luc, Soon Keat Tanb, Ling Zhoua.** Experimental investigation on impingement of a submerged circular water jet at varying impinging angles and Reynolds numbers. *Experimnetal Thermal and Fluid Science.* 2016.

4. **A. Mansourin, H. Arabnejad, S.A. Shirazi, B.S. McLaury.** A combined CFD/experimental methodology for erosion prediction. *Elsevier B.V.* 2014.

5. *A COMPARISON OF CFD SOFTWARE PACKAGES' ABILITY TO MODEL A SUBMERGED JET.* **Alasdair MACKENZIE, A LOPEZ, K RITOS, M T STICKLAND, W M DEMPSTER.** Melbourne, Australia : Eleventh International Conference on CFD in the Minerals and Process Industries , 2015.

6. **Russel M.Cummings, William H.Mason, Scott A.Morton, David R.McDaniel.** *Applied Computational Aerodynamics:A Modern Engineering Approach.* New York NY : Cambridge University Press, 2015.

7. **F.R. Menter, R. Sechner,A. Matyushenko.** Best Practice: RANS Turbulence Modeling . *ANSYS,Inc.* 2021.

8. **Center, Langley Research.** NASA Turbulence Modeling Resource. [Online] NASA. https://turbmodels.larc.nasa.gov/index.html.

9. *Comparison of different turbulence models in pipe flow of various Reynolds numbers.* **Desmond Chin Yoong Lim, Hussain H. Al-Kayiem, Jundika C. Kurnia.** Kuala Lumpur - Malaysia : s.n., 2018.

10. **Online, CFD.** CFD Online. [Online] November 4, 2009. https://www.cfd-online.com/Wiki/RANS-based_turbulence_models.

11. **Menter, Florian R.** Turbulence Modeling for Engineering Flows. s.l. : ANSYS inc., 2011.

12. **Andrew Escue, Jie Cui.** Comparison of turbulence models in simulating swirling pipe flows. *Elsevier.* 2009.

13. **Jonas Bredberg, Shia-Hui Peng, Lars Davidson.** An improved k-ω x turbulence model applied to recirculating flows. *International Journal of Heat and Fluid Flow 23.* 2002.

14. **CFD EXPERTS.** *Ansys Fluent Theory Guide.* Canonsburg : ANSYS,Inc., 2021.

15. **ANSYS Inc.** ANSYS INC AFS ENEA . [Online] ANSYS INC., 1 23, 2009. https://www.afs.enea.it/project/neptunius/docs/fluent/html/th/node81.htm.

16. **STENMARK, ELIN.** On Multiphase Flow Models in ANSYS CFD Software . *Department of Applied Mechanics Division of Fluid Dynamics CHALMERS UNIVERSITY OF TECHNOLOGY.* 2013.

17. **Elshawarby, Omar.** Computational Fluid Dynamics of Multiphase Flow Using ANSYS Fluent . *SCHOOL OF INDUSTRIAL AND INFORMATION ENGINEERING.* 2021.

18. **Mansouri, Amir.** *A COMBINED CFD-EXPERIMENTAL METHOD FOR DEVELOPING AN EROSION EQUATION FOR BOTH GAS-SAND AND LIQUID-SAND FLOWS.* s.l. : University of Tulsa, 2016.

19. **Pasha, A. Hassanpour and M.** Discrete element method applications in process engineering. *Introduction to Software for Chemical Engineers.* 2015.

20. **Théodon, L.** Morphological characterization of aggregates and agglomerates by image analysis: A systematic literature review. *Powder Technology.* 2023, 430.

21. **Yang, J. C. S. Lai and C. Y.** Numerical simulation of turbulence supressions: Comparisons of the performance of four k-ε turbulence models . *Elsevier Science Inc. .* 1997.

22. *CFD Simulation of Turbulent Flow in Pipes Using Different Turbulent Models.* **Dr. Alhadi A Abosbaia, Dr. Abdulhafid M. Elfaghi, Dr. Omar A Almatbage.** 2017.

23. **STENMARK, ELIN.** *On Multiphase Flow Models in ANSYS CFD Software.* Göteborg, Sweden : s.n., 2013.

24. **Elshawarby, Omar.** *Computational Fluid Dynamics of Multiphase Flow Using ANSYS Fluent .* s.l. : POLITECNICO DI MILANO, 2021.